DECADAL VARIABILITY IN THE PACIFIC

E.S. Sarachik and D.J. Vimont, JISAO Center for Science in the Earth System, University of Washington, Seattle, WA., USA

1. Introduction

The last ten or fifteen years have shown remarkable progress in measuring, modeling, and understanding the El Niño/Southern Oscillation (ENSO) phenomenon, its teleconnections to other parts of the world, and its predictability. But ENSO itself has variations on time scales much longer than its intrinsic interannual time scale (two to seven years) and in addition is not the only mode of climate variability that affects the rest of the world. For example, Fig. 1 shows that only three global patterns can explain large amounts of variance of the monthly surface temperature over the United States. Clearly knowing or predicting the state of ENSO, the Pacific Decadal Oscillation (LP in Fig. 1---PDO in the sequel) and the Arctic Oscillation (AO, or in its more familiar guise, the North Atlantic Oscillation, NAO) gives important information about U.S. Climate.

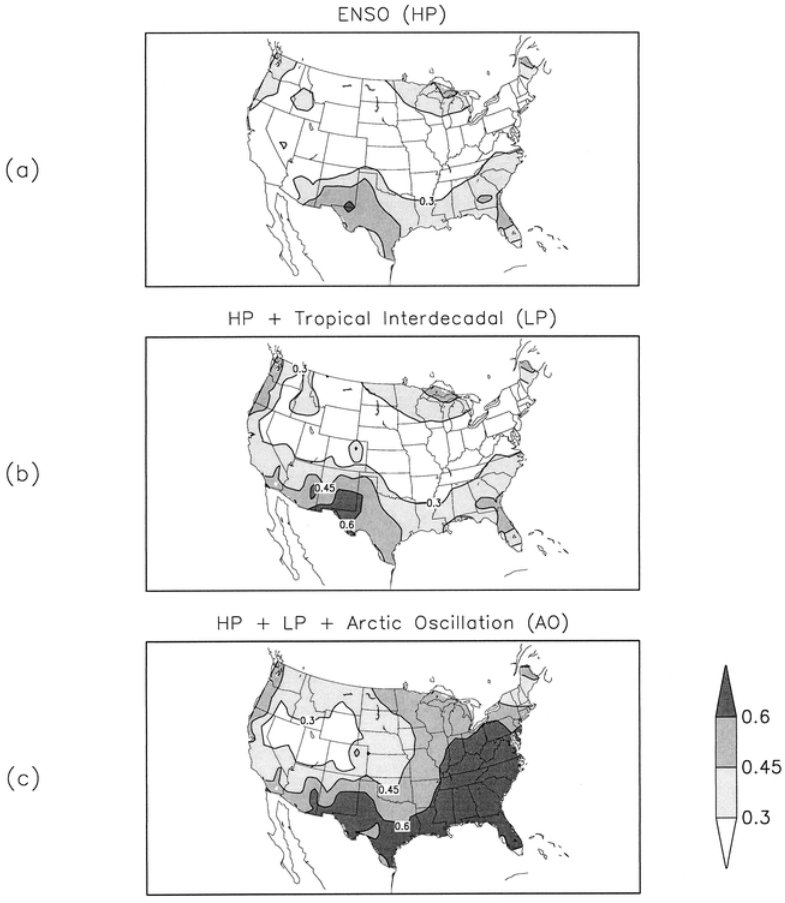

Fig. 1. The 36-yr (1958–93) correlation between time series of JFM observed and JFM reconstructed U.S. surface air temperature. The reconstructed time series are obtained by regressing the observed surface air temperature onto (a) the HP index, (b) the HP and LP indices, and (c) the HP, LP, and AO indices. The critical value of the correlation coefficient (significant at the 95% level) is 0.32. From Higgins et al., 2000.

As we can see from Fig. 1, the west coast of the United States is, not surprisingly, influenced mostly by the ENSO and PDO. A similar picture applies to precipitation, where the effects of both the PDO and ENSO are vividly portrayed in composites of streamflow at the terminus of the great Columbia River of the Pacific Northwest of the United States (Figure 2).

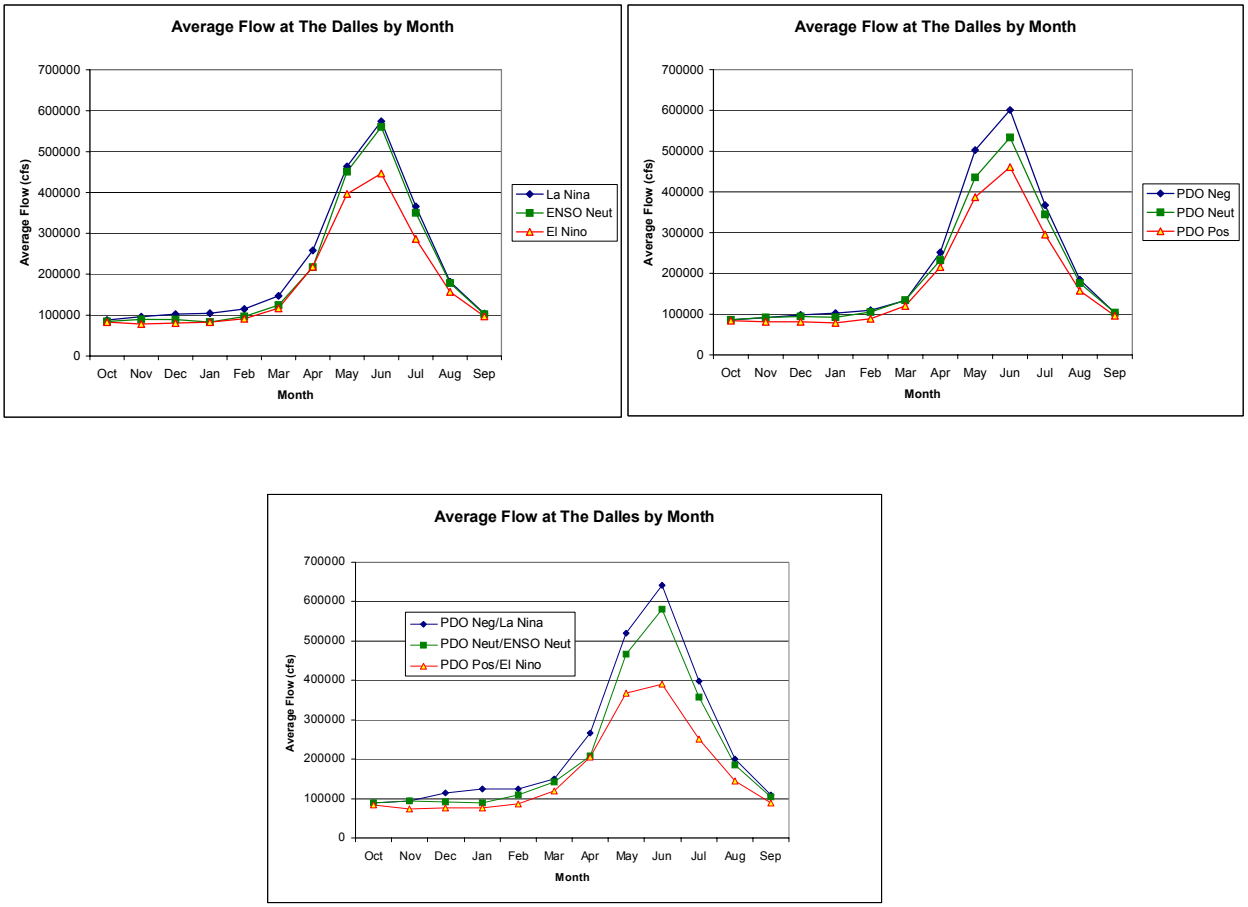

Fig. 2. The monthly flow at the outflow of the Columbia River at The Dalles, Washington, composited by phases of ENSO and PDO and both together From Hamlet and Lettenmaier, 1999.

There are clearly effects of ENSO and PDO separately—when in the warm phase of ENSO or PDO, streamflow tends to be low. When the PDO and ENSO are together in phase (we will see what this means in Section 3), the effects of each are greatly magnified and very low flow conditions obtain for the warm phase of ENSO during a warm phase of the PDO. Clearly the PDO matters for the Pacific Northwest in the same way that the NAO matters for Europe.

There are also indications that Pacific variability is important on the global scale. The well known globally averaged surface temperature shows clear decadal

and interdecadal variability with the major part of the warming over the entire 120 years of the instrumental record. Since fossil fuel emissions have remained continual, the variability of the record (especially the cooling from 1940 to the mid 1970s) must indicate the modulation by decadal climate variability. Further, the sharp increase in warming begins in the mid 1970s, precisely the time that the Pacific was known to undergo a "regime shift."

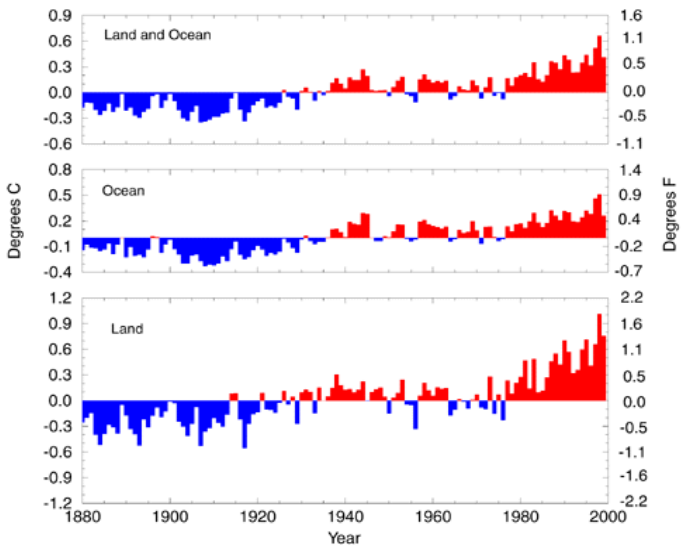

Fig. 3. Annual mean surface temperatures (from the NOAA National Climatic Data Center:
http://lwf.ncdc.noaa.gov/oa/climate/research/anomalies/anomalies.html#means)

We will see later that an important part of the warming since the mid 1970s can indeed be identified with the PDO and the NAO and their unusual tendency to be in the same phase starting in the mid-1970s.

2. Climatology and Normal Patterns of Variability of the Pacific and Overlying Atmosphere

We cannot appreciate decadal variability in the Pacific unless we examine the normal annual cycle. Fig 4. shows the annual cycle of Sea Level Pressure in the Pacific. During (northern) winter, the North Pacific is dominated by a low pressure over and to the southwest of the Aleutian Islands (this feature is termed the Aleutian Low) with a relatively weak subtropical high sitting off California. The subtropical high expands westward in Spring and reaches a maximum in summer (though COADS can't quite resolve it, the southern subtropical high also maximizes in northern summer). The high weakens during autumn as the Aleutian Low begins to strengthen.

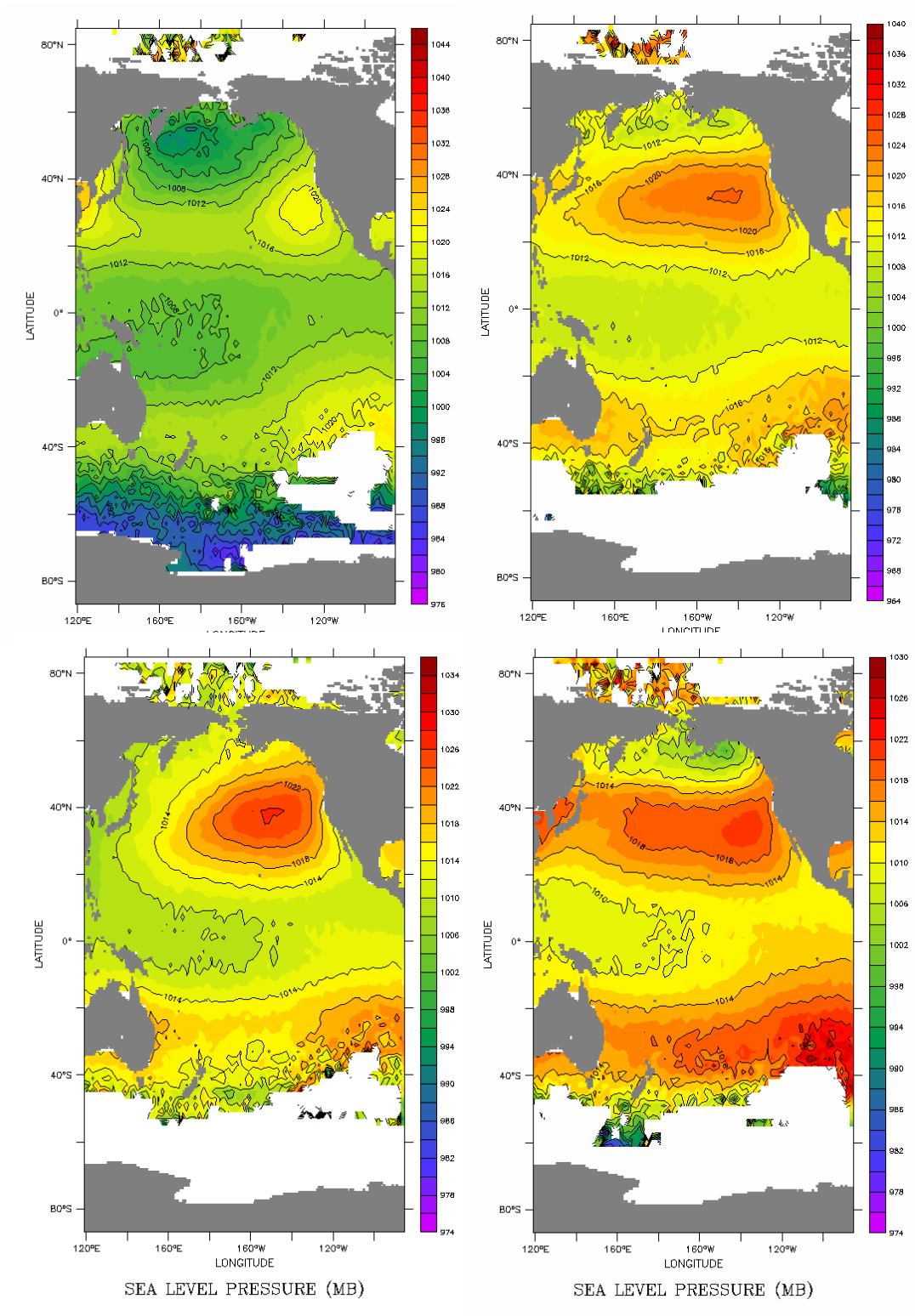

Fig. 4. Climatology of Sea Level Pressure from COADS. Upper Left: Jan, Upper Right: April, Lower Left: July, Lower Right: October. From http://ferret.wrc.noaa.gov/las/main.pl

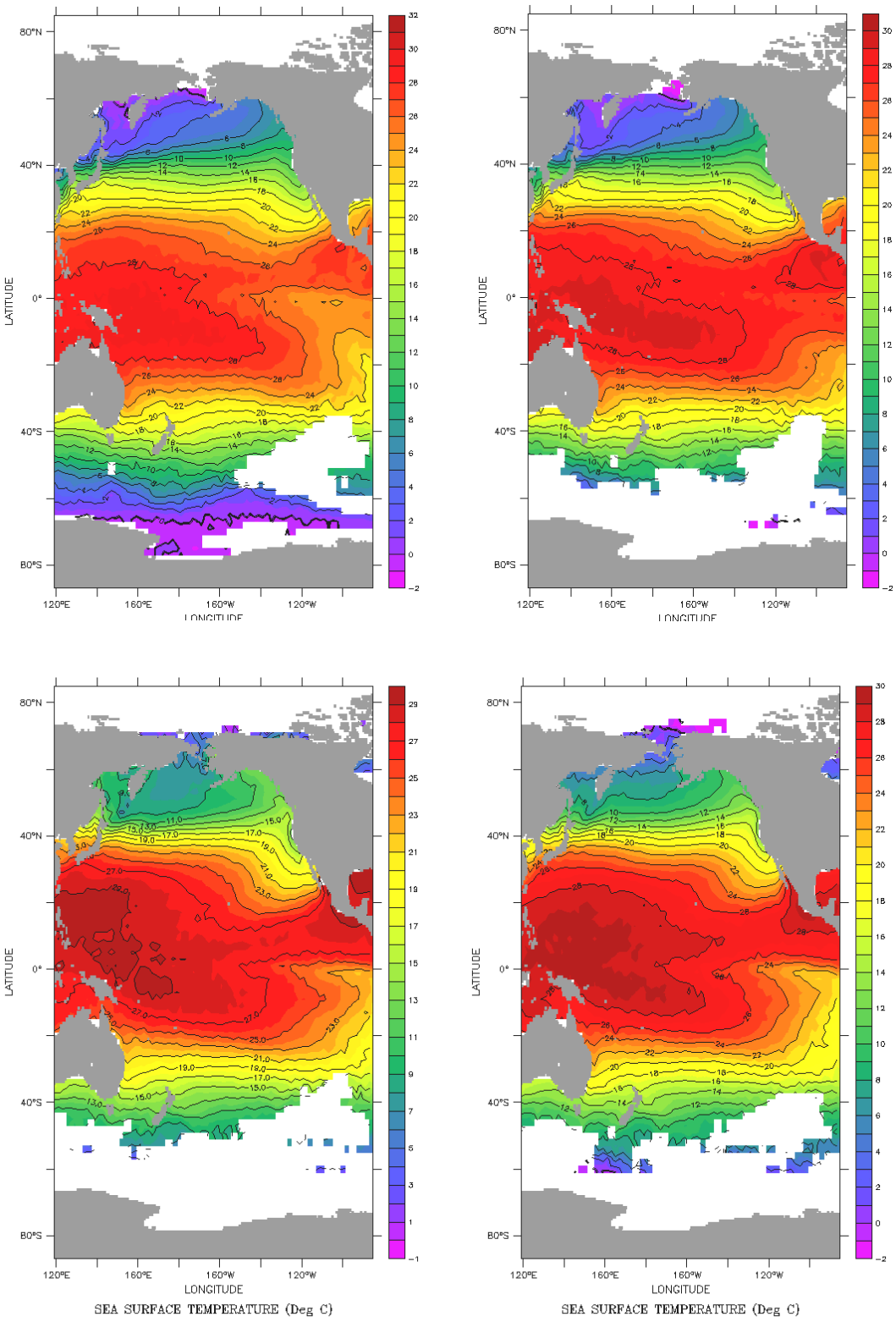

Fig. 5. Sea Surface Temperature from COADS. Upper Left: Jan, Upper Right: April, Lower Left: July, Lower Right: October. From http://ferret.wrc.noaa.gov/las/main.pl

Fig 5 shows the climatology of SST. North Pacific SST is of course cold in winter and warm in summer. Equatorial SST has a quite different climatology: it is warmest in (northern) spring and coldest during autumn, with a minimum in the eastern Pacific. As seen in Fig. 5, equatorial SSTs in the eastern and central Pacific tend to be slightly cooler than off-equatorial SSTs, due to the presence of upwelling along the equator. The region of cool equatorial SST that extends from the eastern Pacific to about the dateline is referred to as the "cold tongue". In the northern mid-latitudes near 40°N a strong meridional SST gradient is observed off the west coast of Japan. This gradient marks the Kuroshio-Oyashio Extension (KOE), an eastward ocean current that denotes the boundary between the subtropical (clockwise) and subpolar (counter-clockwise) gyres.

Normal conditions in the tropical regions have the western Pacific SST warm with heavy rainfall over the warm water (Fig 6a). The rainfall exists because the moist air is, in general, rising over warm water and condenses as it rises: this produces low SLP over the western Pacific. The descending air sinks in the eastern Pacific and SLP is high there. The surface trade winds are to the west from high pressure in the east to low pressure in the west. Every few years in the Equatorial Pacific, conditions change radically. Fig 6b shows warm conditions in the Tropical Pacific (the warm phase of ENSO, commonly called El Niño). The warm water expands eastward, the region of heavy precipitation follows the warm water, and the SLP in the west rises while the SLP in the east falls. The westward winds get weaker and sometimes reverse entirely to eastward. During cold phases of ENSO, Fig. 6c, the warm water contracts westward, cold water in the east expands westward, the westward winds intensify, and SLP weakens in the west and increases in the east. The cycle of ENSO, as measured by the so called NINO3 index of averaged temperatures from 90°W to 150°W, 5°S to 5°N is shown in Fig 6d to indicate the interannual nature of the warm and cold phases of ENSO.

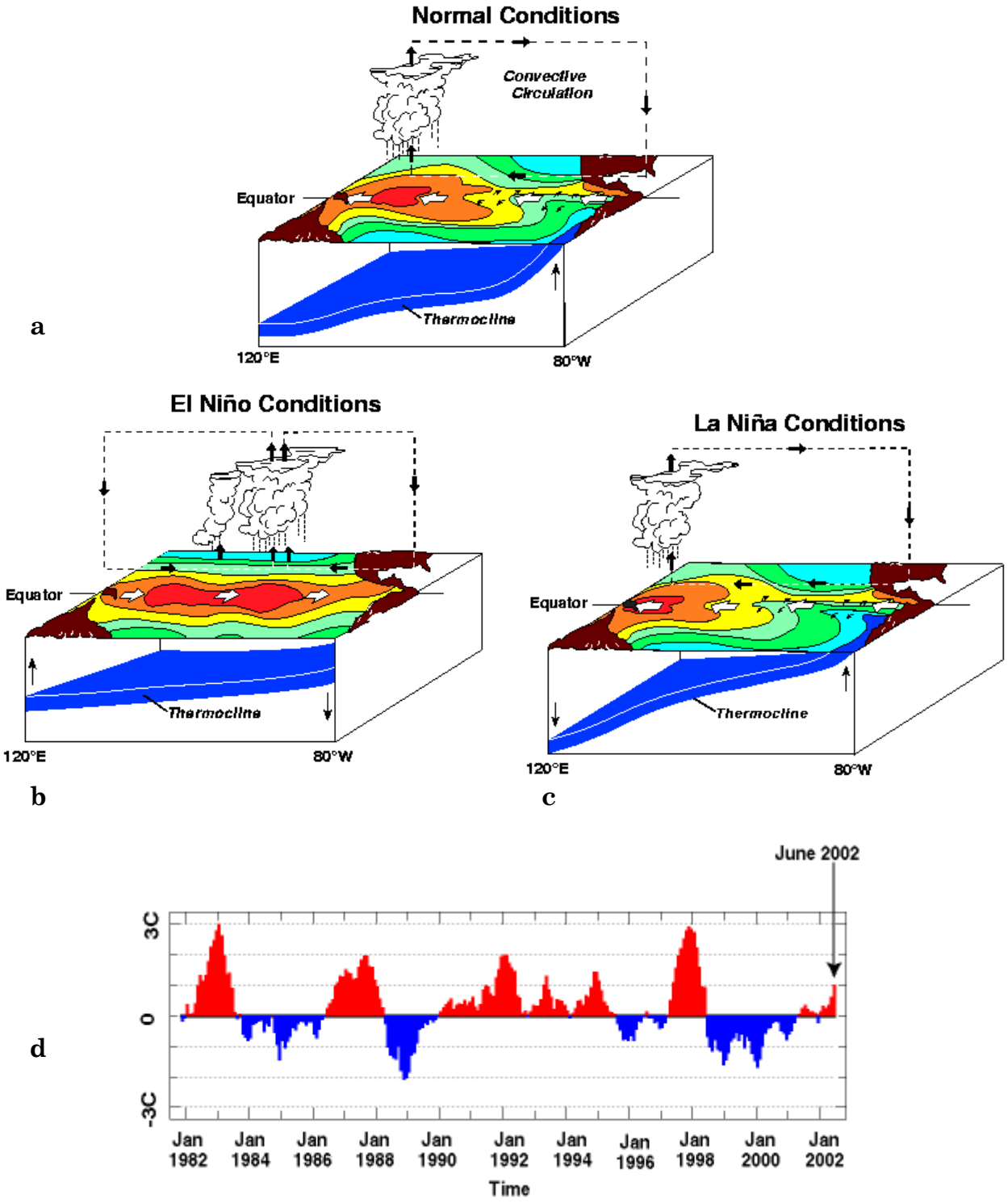

Fig 6. a: Normal conditions in Tropical Pacific. b: Warm Phase of ENSO. c: Cold Phase of ENSO. d: Recent time series of East Pacific temperatures.
From NOAA PMEL http://www.pmel.noaa.gov/tao/elnino/nino-home.html#

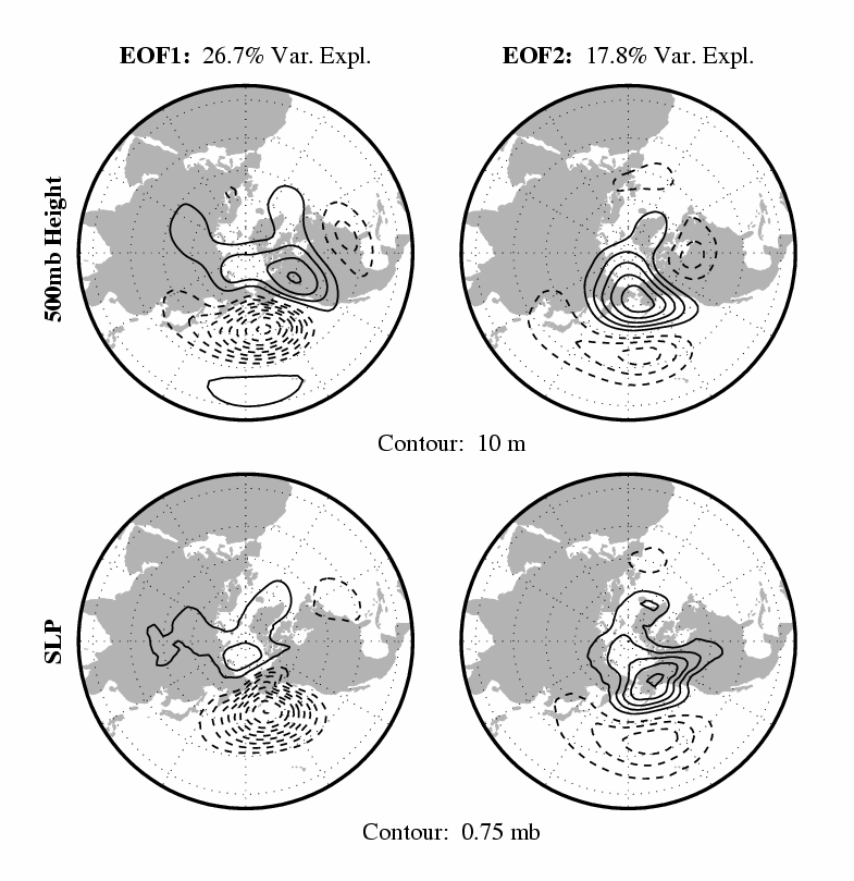

Fig. 7. Modes of atmospheric variability. Top row: EOF1 (left) and EOF2 (right) of monthly wintertime (ONDJFMA) 500mb height over the Pacific. Patterns are generated by regressing 500mb height onto the associated principal component time series. Bottom row: SLP regressed onto the principal component time series from the top row. For all maps, solid contours denote positive values, dashed contours denote negative values, and the zero line has been omitted.

The dominant modes of low-frequency (> 10 days) mid-latitude atmospheric variability over the Pacific include the Pacific North American (PNA) pattern, and the West Pacific (WP) pattern. These patterns are shown in the first two EOFs of monthly wintertime (ONDJFMA) 500mb height over the Pacific in Fig. 7. The leading EOF is the PNA pattern, which consists of a wave train with centers over the tropics, the Aleutian Low, the northern US and Canada, and Florida. The second EOF identifies the West Pacific (WP) teleconnections pattern, with centers over the central Pacific, and over the Baring Sea. These patterns have been identified in numerous analyses, such as Wallace and Gutzler (1983), and Barnston and Livezy, (1987).

The surface patterns that accompany the PNA and WP patterns are shown in the bottom row of Fig. 7, which shows the regression maps of SLP onto the PNA and WP time series (the principal components associated with EOF1 and EOF2). SLP anomalies associated with the PNA pattern (bottom left) include variations in the strength of the Aleutian Low (the climatological feature in Fig. 4). For the WP pattern, the surface SLP anomalies consist of a dipole on either side of 45°N with centers over Alaska and over the climatological subtropical high in Fig. 4. The SLP pattern in the lower right panel of Fig. 7 has been termed the North Pacific

Oscillation (NPO) by Walker and Bliss (1932). Connections between the upper-level 500mb height variations and the surface SLP variations have been investigated by Hsu and Wallace (1985).

3. Decadal Patterns in the Pacific Ocean and Overlying Atmosphere

SST is the longest continuous instrumental record from which to construct records of decadal variability over the Pacific. This is usually done from either the COADS data set (Woodruff et al, 1987) which is most usable for global coverage from 1950 to the present, or the U.K. Meteorological Office Historical Sea Surface Temperature Dataset (Folland and Parker, 1990, 1995). The advantage of the COADS set is that the associated parameters of winds, humidity, and clouds are available to construct fluxes and other quantities which can help interpret the SST variability. Another commonly used data set is the NCEP Reanalysis (see Kalnay et al. 1996), which assimilates observed data into an atmospheric model. The resulting model output includes complete spatial and temporal coverage from 1948 to present times, but suffers from some assumptions that are built into various model parameterizations.

It is unfortunately true that there have been a number of analyses that differ enough in method and/or domain that it is difficult to compare and interpret the various studies. Some use annual data and some winter, some use global data and some use only north Pacific, while some use empirical orthogonal functions (EOFs) and some rotated EOFs to maximize the variance explained, and some give only the leading EOF which may be another analyst's second or third EOF. We will try to present the various studies coherently to indicate not only the variability, but also to point to the underlying dynamics that produces the variability.

Fig 8 shows the first two EOFs for the *wintertime* SSTs in the Pacific north of 20°S, from Deser and Blackmon (1995). The first EOF is dominated by the usual ENSO signal, with the time series of the principal component showing predominantly interannual variability and the major warm and cold phases of 1965/6, 1972/3, 1982/3, and the continuing warmth of the early 1990s. The cold region in the North Pacific centered at 160°W, 30°N is a well known concomitant to warm ENSO phases along the equator. Note that it is of opposite signs to SST both at the Asian and North American coasts. The second EOF, Fig 8B, has most of its amplitude along 40°N, is zonally elongated, and has much weaker connections to the equatorial region. It is connected to the Asian coast at Japan but is of opposite sign at the North American coast. Its time series is mostly decadal.

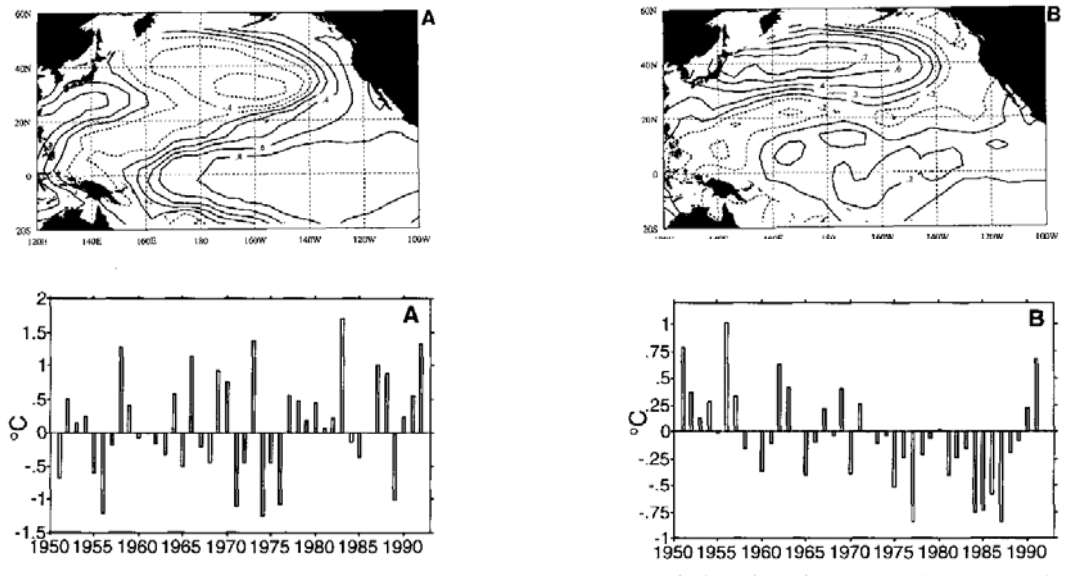

Fig. 8. First two EOFs of winter (November to March) SST in the Pacific north of 20°S. From Deser and Blackmon, 1995.

Though the time series in Fig. 8a is primarily interannual, it also clearly exhibits longer, decadal-scale variations. Similarly, the predominantly decadal time series in Fig. 8b also contains variability with shorter, interannual time scales. A recurring problem in studies of decadal variability is the search for a clean, physically meaningful method of dividing the variability by time scales.

Zhang, Wallace and Battisti, 1997, examined the time dependence of such variability simply by comparing patterns of SST variability in 6 year highpass, or lowpass filtered data. The leading EOFs of highpass and lowpass filtered SST north of 30°S are shown in Fig. 9. We see that the patterns share many of the same characteristics, implying that the low frequency pattern may simply reflect the low frequency variability of ENSO since lower frequency focing of the ocean leads to wider meridional extent of the ocean response (Cane and Sarachik, 1981).

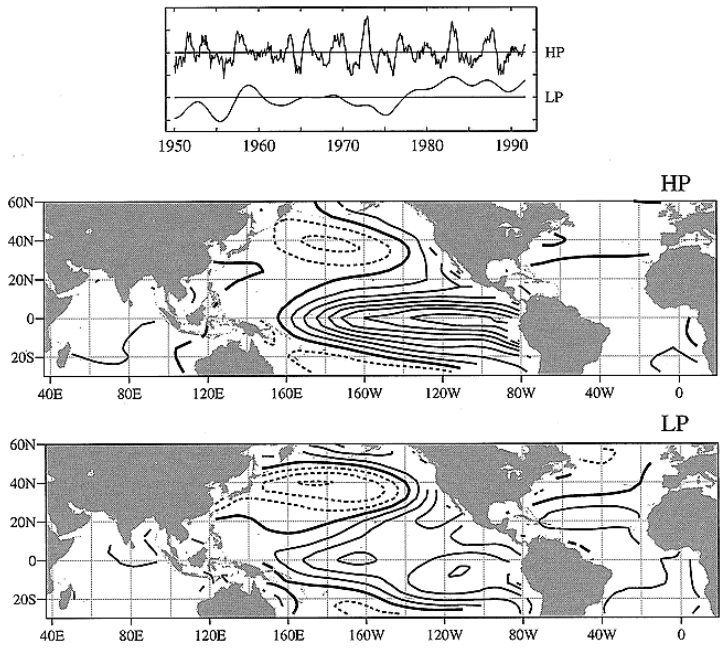

Fig. 9. High passed and low passed EOFs (annual data) for the Pacific north of 20°S. The time series is then regressed on the global SST (From Zhang, Wallace and Battisti, 1997).

It should be noted that if the EOF is taken only for unfiltered Pacific SSTs north of 20°N, and the time series of that north Pacific EOF is then regressed on the global SST, we get what has come to be known as the Pacific Decadal Oscillation (PDO; Mantua et al, 1997) as shown in Fig. 10. Note that the PDO shares many features of the lowpass-filtered results of Zhang et al. (1997) in Fig. 9, though the PDO exhibits larger amplitude cooling along 40°N, like Deser and Blackmon's EOF2. Since no time filtering is used, the PDO also has interannual variability which exists in the SST of the North Pacific, possibly forced by the high and low frequency variability of ENSO.

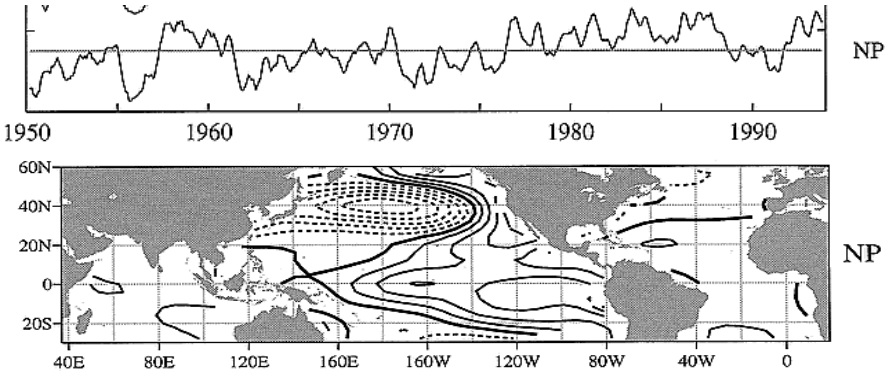

Fig. 10. Upper diagram: the time series for the EOF of North Pacific SST. Lower diagram: the regression of the NP index on global SST. From Zhang, Wallace, and Battisti, 1997.

Because surface variables are part of the reanalysis data set (see Kalnay et al, 1996) the suite of ocean surface variables that accompany the high and low frequency patterns in Fig. 9 can be obtained. A representation of the ENSO pattern can be obtained by averaging the SST over the eastern equatorial Pacific (over the region 6°S—6°N, 180°—90°W): this series is called the cold tongue index, CT. Zhang et al. (1997) construct two time series that represent the high- and low-frequency modulation of ENSO. The first, labeled CT*, is defined by applying the 6 year highpass filter to the CT index. The second is defined by calculating the first principal component (PC) of global SST north of 30°S, fitting CT* to that PC (by a linear least-squares fit), and removing the fitted time series from that leading PC. This second time series is labeled the "global residual" (GR) time series, and represents the dominant pattern of "residual" global SST variability that remains after interannual ENSO variability has been removed. These two time indices are plotted in Fig. 11.

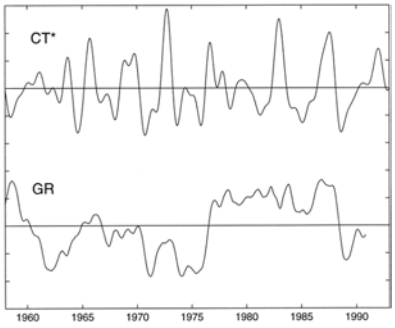

Fig. 11. The cold tongue and global residual time series from Zhang et al., 1997 as given by Garreaud and Battisti, 1999.

The CT* is very similar to the High Pass (HP) index in Fig. 9 and gives a good representation of the ENSO index. Similarly the GR index is similar to the NP index of Fig. 10 and to the LP index of Fig. 9. The steep change of the GR index in 1976 has been related to the "regime shift" of 1976 that has been dealt with by Trenberth (1990), Trenberth and Hurrell (1994) and Miller et al., 1994. While in the sequel we will not consider regime shifts as a quantity distinct from the variability of decadal patterns, we do note that there is some evidence for sudden shifts in the equatorial thermocline (Guilderson, and Schrag, 1998) and in biological time series in 1976 and 1989 (Hare and Mantua, 2000)--note that these latter periods are times of rapid change of the GR index in Fig. 11.

Fig. 12 shows the surface variables that coincide with the ENSO-like mode. It is apparent that the variability is generally symmetric about the equator lending even more support to the idea that the mode is mostly a low frequency forcing by the low frequency part of ENSO. The sea level pressure signal shows the surface manifestation of the Aleutian low while the winds seem to indicate additional low

frequency convergence to the south-east of Indonesia that did not exist in the high frequency ENSO forcing.

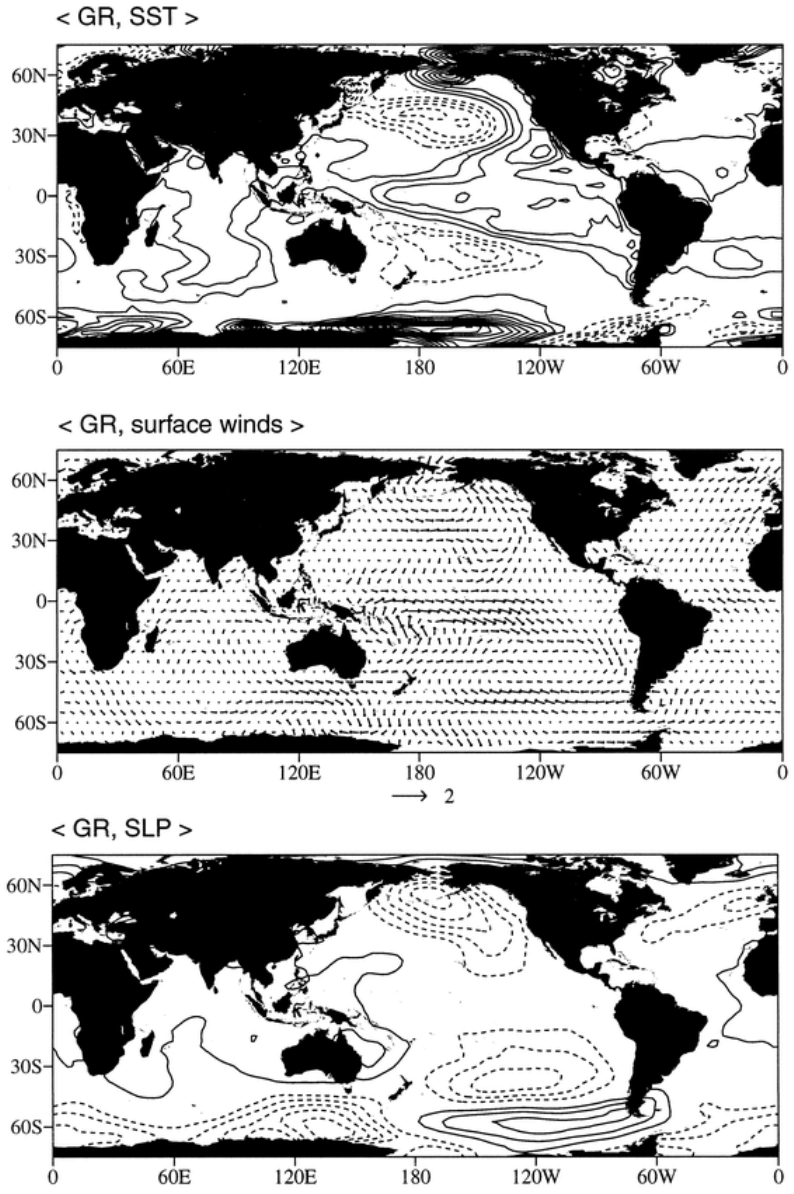

Fig. 12. Annual SST, surface winds and sea level pressure regressed on the GR index of Fig. 7. From Garreaud and Battisti, 1999.

So far the evidence indicates that the decadal SST in the North Pacific is consistent with being driven from the tropics by the low frequency variability of ENSO. Evidence that something more is going on comes from careful analyses of SST in the North Pacific.

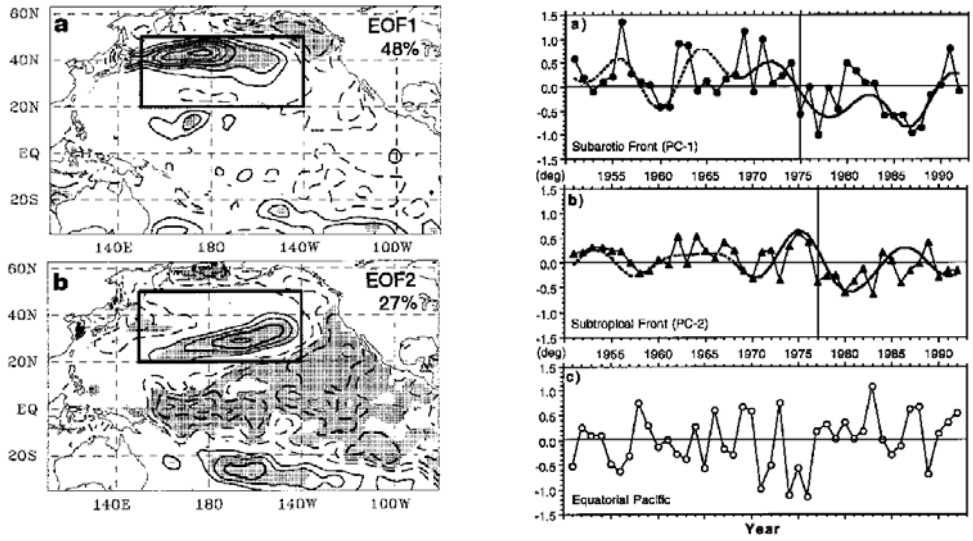

Fig 13. Left: First two EOFs of decadally filtered SST in box in North Pacific and correlation of the time series of the given EOF with the rest of the Pacific. Right: Time series of the EOFs (from Nakamura, Lin, and Yamagata, 1997).

The first EOF lies along 40°N and extends to the coast of Japan. It lies along the subarctic front and its EOF has almost no correlation with the rest of the Pacific. The second EOF looks very much like the pattern that goes with the ENSO-like mode of Fig. 12. The two time series indicate that in the mid-seventies, cooling in the North Pacific (EOF1) tends to lead warming in the tropics (EOF2), so that EOF mode 1 does not appear to be forced by the tropics.

The seasonality of the North Pacific SST (shown in the maps of root-mean-squared winter and summer SST variability in Fig.14) may play an important role in explaining Pacific decadal variability. This seasonality is somewhat surprising since the SST anomalies appear to be greater in summer than in winter.

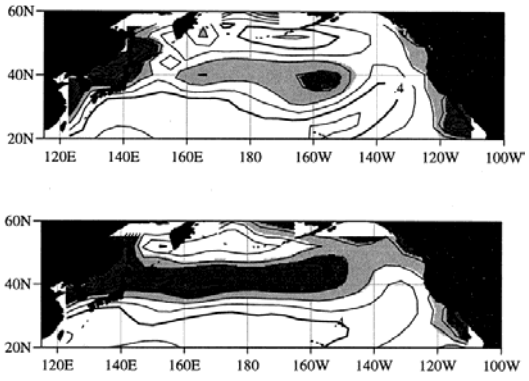

Fig. 14 Top Panel: The rms SST variability (on all time scales) for winter. Bottom Panel: The rms SST variations for summer. From Zhang, Norris and Wallace, 1998.

The EOFs of North Pacific SST taken separately for summer and winter are shown in Fig. 15. Note from Fig 15 that the summertime pattern looks very much like the first EOF in Fig. 13 except that the opposite signed piece of the pattern extending from Baja California southwestward into the tropics is much emphasized in the summertime pattern.

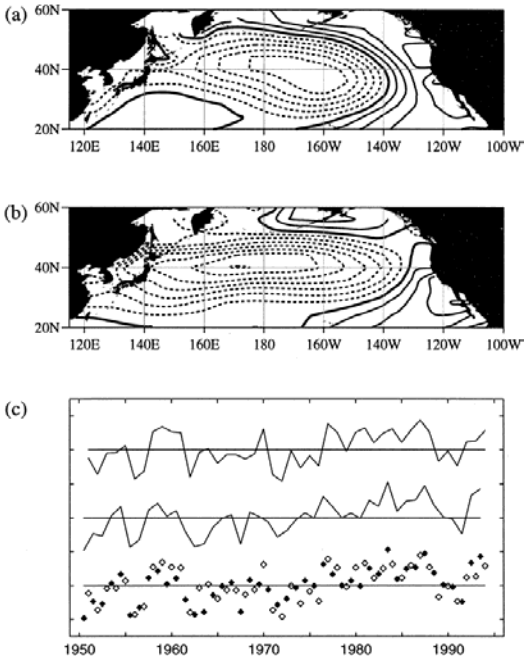

Fig. 15 (a) Leading EOF for SST for winter. (b): Leading SST EOF for summer. (c): Time series for winter and summer EOFs and, in the third row of (c), both, with summertime being filled diamonds. From Zhang, Norris, and Wallace, 1998.

Visual inspection of the time series of Fig. 13 indicates that the cooling in the mid seventies had the EOF1 leading the cooling associated with the ENSO like variability so that the EOF1 mode seems *not* to be forced by the tropics. This is validated by an explicit attempt to remove all ENSO correlations from the SST field and examine the residual. In Zhang et al, 1996, an annual ENSO index was defined and correlated with both the SST and the 500mb field. The result is the usual ENSO pattern and its atmospheric counterpart which is shown in the left hand panel of Fig. 16 Note that the atmospheric 500mb pattern resembles but is not quite the PNA pattern. The ENSO variability is then removed from the SST and 500mb height fields (via linear regression), and the leading patterns of covariability between these "residual fields" are identified using SVD analysis. These patterns are shown in the right panel of Fig. 16. This panel, which has had ENSO linearly removed, bears some resemblance to the sub-arctic SST variability of Fig. 13, and the 500mb chart is more nearly PNA. Insofar as possible, ENSO at all frequencies has been removed and, as expected, what remains is not at all ENSO like. It too has the main SST field extending all the way westward to Japan and has hints of the southwest structure off the coast of Baja California.

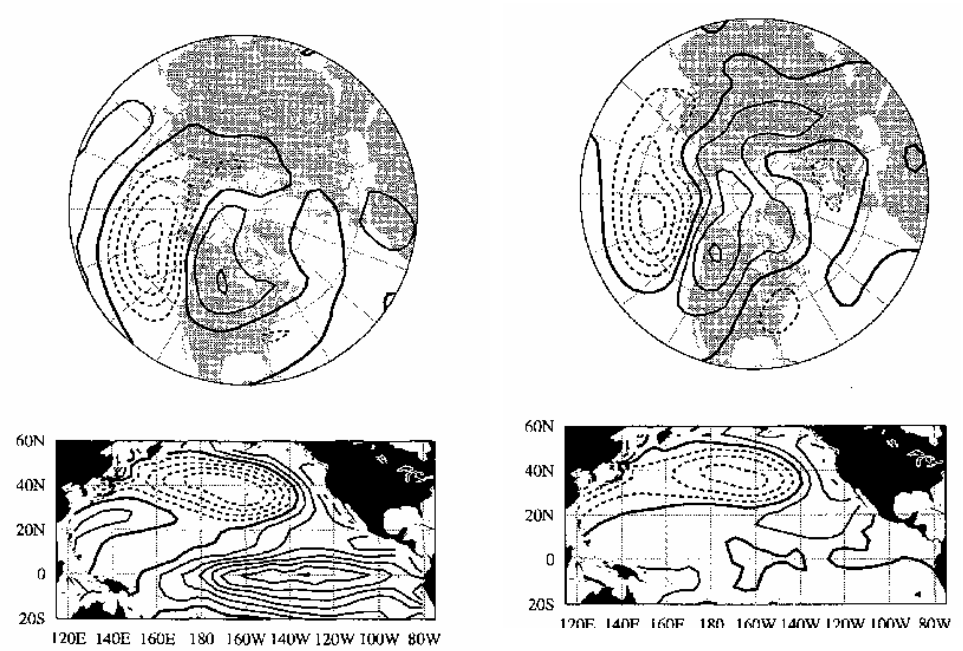

Fig. 16. Left Panel: Leading SVD fields of SST and 500mb height Right Panel: leading SVD fields of SST and 500mb fields where ENSO has been removed (From Zhang, Wallace, and Iwasaka, 1996).

Finally we note the work of Barlow et al, 2001 who looked at rotated EOFS through the entire Pacific north of 20°S. Fig 17 shows the first three rotated EOFs and their time series using data for the entire year contrasted for the corresponding EOFs calculated only from summer data. We see many of the same features as before but now it is clear that all the previous modes indeed exist throughout the summer. ENSO naturally appears as the first rotated EOF and has predominantly interannual variability. A PDO-like pattern appears naturally as the second REOF with a predominantly decadal time series. The North Pacific SST expression of this PDO-like pattern has considerably less amplitude than the defining picture for the PDO in Fig. 10 would lead one to expect. The North Pacific mode appears as a separate mode quite like the non-ENSO influenced mode in Fig. 16. The time series for the North Pacific mode is similar to the EOF1 mode of Fig. 13. It has distinct correlations with precipitation over the US that differs from the PDO: Barlow et al therefore make a strong case that it is a mode of variability that needs to be considered in addition to the PDO. The time series for the North Pacific mode in Fig 16 is similar to the EOF1 mode if Fig. 13.

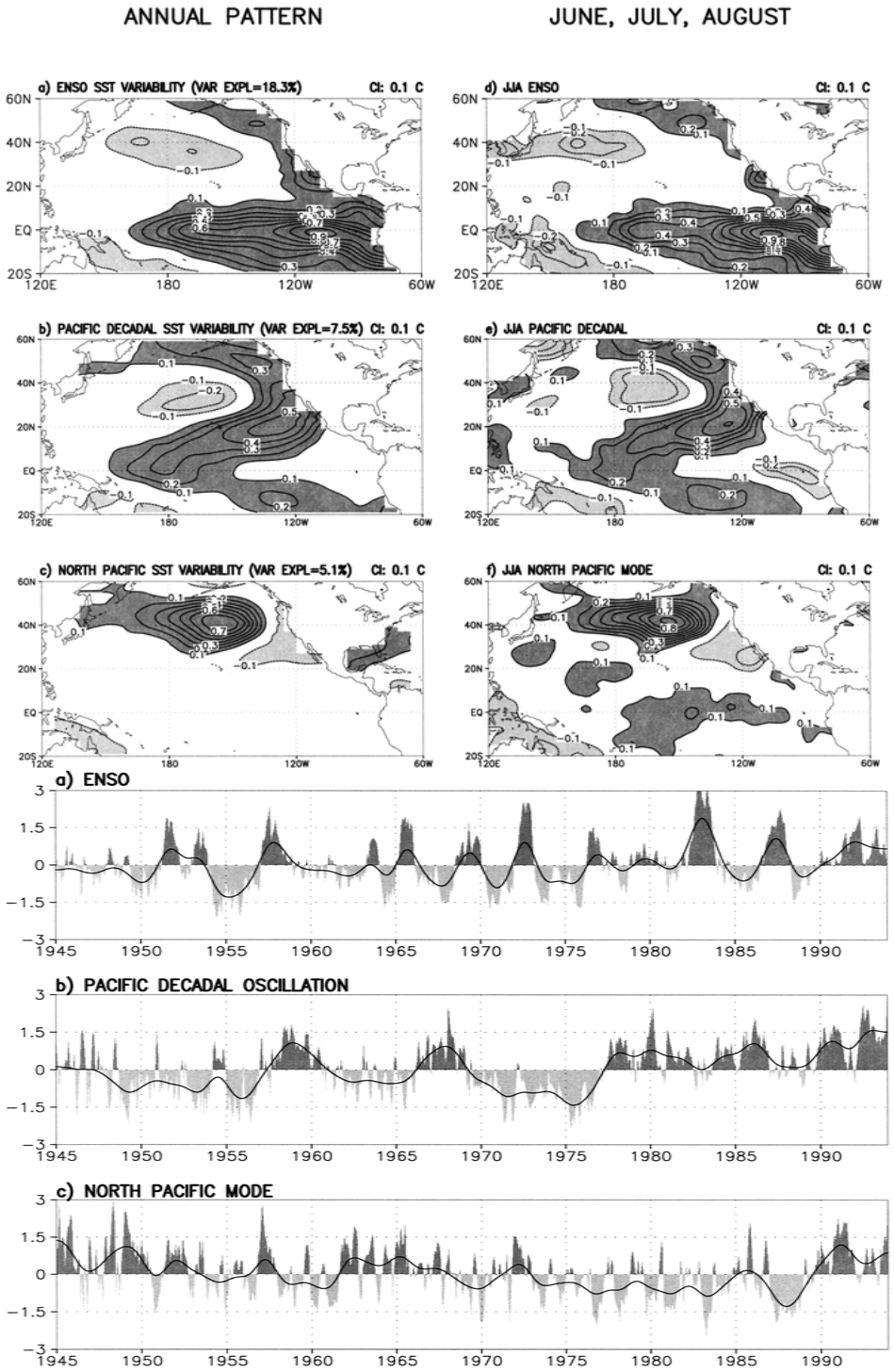

Fig. 17 Leading Rotated EOFs for Pacific. a)First REOF corresponding to ENSO, b) second REOF corresponding to the PDO c) Third REOF corresponding to a different mode here called the North Pacific mode. The contouring is such that it corresponds to one standard deviation of the time series. From Barlow et al, 2001.

Having introduced the various SST modes of variability, we promised to address the relationship between these decadal modes and the increase of globally

averaged surface temperature in Fig. 3. It was Wallace and collaborators (Wallace, Zhang, and Renwick, 1995; Wallace, Zhang, and Bajuk, 1996) who noticed that 1). The surface warming during the northern winter was larger than the warming during the summer especially since 1976 and 2). The pattern of the warm surface anomalies had the northern continents warm and the oceans cool---the COWL (cool ocean warm land) pattern. The arguments are well summarized in Wallace, 1996.

Fig 18. The wintertime correlations of temperature anomaly with NAO (top panel), PDO (middle Panel) and ENSO (lower panel) over the time period 1935-1994. From Hurrell, 1996.

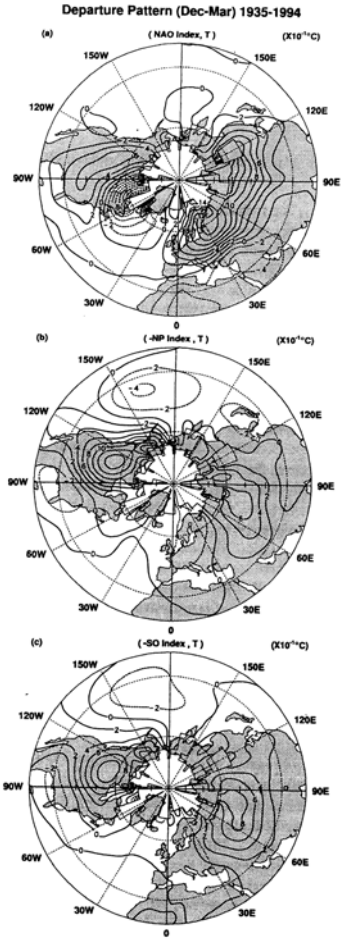

Hurrell (1996) went further and showed that the correlations of ENSO, NAO and PDO with surface temperature gave the same high latitude warming as the COWL pattern (Fig 18) which therefore has the following interpretation: the reason for the enhanced winter warming was the unusual in-phase behavior of the NAO and PDO patterns since 1976. The inevitable implication is that one cannot

understand global warming without understanding the basic patterns of low frequency variability.

4. Mechanisms for the Persistence of SST

We have seen that there is decadal variability during both summer and winter. In order for decadal SST signals to exist, there must be some mechanism to allow SST anomalies to persist from one winter to the next and from one summer to the next. We will examine two mechanisms proposed to increase the persistence of North Pacific SST mechanisms.

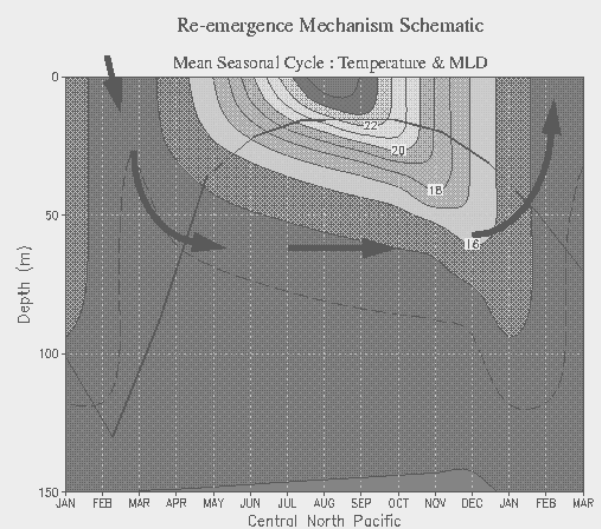

Fig. 19. Schematic of re-emergence mechanism. From Alexander, Timlin, and Scott, 2001.

The mechanism for persisting through the winter was elucidated by Alexander and Deser, 1995 and by Alexander, Deser and Timlin, 1999 and is shown in Fig. 19. During the summer, a strong shallow mixed layer forms in the North Pacific. Any anomaly that formed in the deep mixed layer of the previous winter is trapped under the newly formed summer mixed layer and simply stays there during the entire summer. As the following winter sets on, the mixing due to storms and winter cooling mixes away the summer mixed layer and reveals the previous winter's anomaly to the surface.

The mechanism for persisting through the summer is entirely different and depends on a positive feedback between SST and low clouds (Norris, Zhang, and Wallace, 1998). The basic analysis showed that cool SST anomalies had increased amounts of low level stratus thereby reinforcing the original cold SST by reducing the downward solar radiation at the surface. Similarly, warm SST anomalies had less low level clouds thereby reinforcing the warm water. This mechanism only

seems to work in the calm of summer where the low level stratus is not disturbed by winter storminess.

5. Mechanisms of Decadal Variability

Due to the short duration and limited spatial coverage of the observational record, theories of decadal variability have been heavily influenced by investigations of long simulations of coupled general circulation models. This section presents some leading theories of decadal variability derived from physical arguments, and from GCM simulations. Whenever possible, we attempt to present the observational and model evidence for the existence of these mechanisms. Readers may wish to consult a more comprehensive review by Miller and Schneider (2000).

5.1 Mechanisms of tropical decadal variability

The strong similarities in the spatial structures of tropical interannual and decadal variability (c.f. Fig. 9) lead to a default assumption that tropical decadal variability may be described by similar dynamics as interannual variability. It is generally accepted that interannual ENSO variability is governed by the delayed oscillator mechanism. We begin this section with a brief overview of the delayed oscillator mechanism and its implications for decadal variability. Following the overview, we discuss some viable variations to the delayed oscillator mechanism that have been proposed to explain tropical decadal variability.

The delayed oscillator mechanism (Battisti and Hirst, 1989) may be interpreted as the statement that an ENSO event, once initiated, contains within it a means for its own amplification (a positive "Bjerknes feedback"), as well as the seeds of its own destruction some time later (a delayed negative "ocean memory feedback") (see Neelinet al., 1998, for a review). Although these feedbacks contain a rich mixture of processes, they may generally be described as follows. Consider, in the case of the warm phase of ENSO in Fig. 6, an initial relaxation of the climatological westward trades. Part of the ocean adjustment to these relaxed trades consists of an eastward propagating Kelvin-wave signal, which will tend to depress the thermocline in the eastern and central Pacific, and warm the surface via a decrease in the amount of cool water that is upwelled to the surface from beneath the thermocline. The resulting SST increase in the eastern Pacific reduces the climatological zonal temperature gradient along the equator, to which the atmosphere responds with a further reduction in the strength of the trades. This cycle completes the positive Bjerknes feedback for the delayed oscillator mechanism. At the same time the relaxed trades force uncoupled, westward-propagating Rossby-wave signals that, upon reaching the western ocean boundary, reflect as an upwelling Kelvin wave. This upwelling Kelvin wave counters the positive Bjerknes feedback in the central Pacific and provide the negative ocean memory feedback that eventually terminates the El Niño event.

Though the delayed oscillator mechanism produces tropical variability with a preferred interannual time scale, it is also capable of generating variance across a wide range of time scales, including decadal. The nature of the decadal variability produced by the delayed oscillator mechanism is closely tied to the stability of the delayed oscillator mode, or ENSO mode. In the early models of ENSO (e.g., Zebiak and Cane, 1987; Battisti, 1988; Battisti and Hirst, 1989; Schopf and Suarez, 1988), the delayed oscillator mechanism produces self-sustained oscillations due to a linearly unstable ENSO mode. For some parameter regimes, interactions between the annual cycle and this unstable ENSO mode lead to chaotic model behavior, including a rich temporal structure of variability that may include decadal spectral peaks (Chang et al., 1995; Tziperman et al., 1995; Cane and Zebiak, 1995).

Recent studies using more "realistic" parameters produce a linearly stable ENSO-mode, from which interannual and decadal variance is maintained by energy input from stochastic forcing (Chang et al., 1996; Thompson and Battisti, 2001). Fig. 20 shows the range of spectral estimates of tropical variability produced by the linear stochastic ENSO model of Thompson and Battisti (2001), as well as the spectrum of observed variability. The variance spectrum of observed tropical decadal variability is well within the bounds of the linear model's ENSO variability, suggesting that observed tropical variability may be no more than the decadal residue of the delayed oscillator mechanism. We note that in general, the spectra produced by the stochastically forced linearly stable models produce more realistic spectra at decadal time scales than the chaotic models, though the observational record is too short to definitively establish whether ENSO is in a linearly stable or unstable regime in nature. In either case, the delayed oscillator mechanism is clearly capable of generating realistic levels of decadal variance.

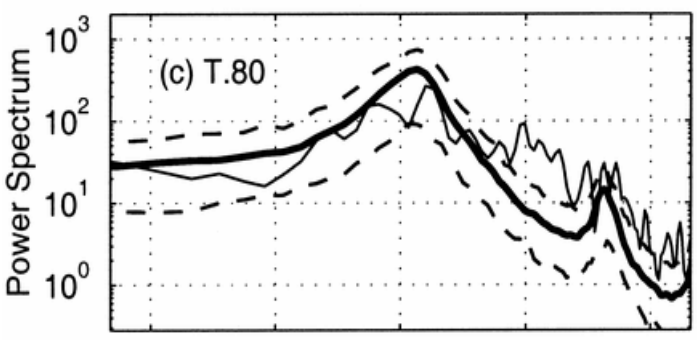

Fig. 20. Power spectra of ENSO variability from the linear stochastic model of Thompson and Battisti (2001): model (thick solid line), observed COADS data (thin solid line), range of spectral estimates obtained by taking individual 42-year sections (the length of the COADS data) of the model NINO3.4 index (thin dashed lines). From Thompson and Battisti (2001)

Various forms of the delayed oscillator mechanism have been invoked to explain tropical decadal variability in some GCM simulations. Kirtmann (1997)

shows that the dominant time scale of tropical variability produced by the delayed oscillator mechanism is sensitive to the meridional structure of coupled zonal wind stress anomalies in the central Pacific. The meridionally broadened zonal wind stress anomalies project onto higher order (meridional) Rossby waves, which weaken the negative ocean memory feedback through reduced Kelvin wave reflection efficiency off the western boundary (Cane and Sarachik, 1977). This mechanism has been invoked to explain tropical decadal variability in the GCM simulations of Knutson and Manabe (1998).

Similarly, Liu et al. (2002) show that higher order (vertical) modes (and hence slower wave propagation speeds) may be responsible for producing decadal tropical variability in a coupled ocean atmosphere model. In a 1000 year simulation of the CSIRO CGCM, Vimont et al. find that while the positive Bjerknes feedback operates on both interannual and decadal time scales, the negative ocean memory feedback is absent on decadal time scales. The existence of the positive Bjerknes feedback on decadal time scales implies that coupled dynamics will tend to amplify the tropical response to forcing on decadal time scales, and will produce a similar spatial structure of variability as the interannual ENSO variability regardless of the source of the forcing.

5.2 Mid-latitude variability

Mid latitude variability may generally be viewed as the superposition of intrinsic mid-latitude variability, and externally forced mid-latitude variability (by, say, tropical ENSO variability). In this section, we discuss mechanisms of intrinsic mid-latitude variability, though many of these mechanisms may also apply in the presence of external forcing.

5.2.1 Stochastic processes

The large disparity in time scales of atmospheric (days to weeks) and oceanic (months to years) processes gives rise to a powerful set of stochastic models with which to describe mid-latitude climate variability. In these models, the non-linear atmospheric dynamics that give rise to day-to-day weather fluctuations may be parameterized as a stochastic white noise process.

A simple yet powerful example of a stochastic climate model is proposed by Hasselmann (1976), and used by Frankignoul and Hasselmann (1977) to describe the passive thermal response of the oceanic mixed layer to stochastic heat flux and momentum forcing from the atmosphere. The model may be written:

$$\frac{dT_o}{dt} = f(t) - \lambda T_o, \qquad (1)$$

where f(t) is the stochastic atmospheric forcing, and T_o is the ocean temperature anomaly response that integrates the forcing, and damps with an e-folding decay

time λ^{-1}. The damping time scale λ^{-1}, is proportional to the depth of the oceanic mixed layer (and hence its thermal inertia), and ranges between three and six months for the initial rate of decay of mid-latitude SST anomalies (Lau and Nath, 1996; Deser et al., 2002).

The behavior of the Hasselmann (1976) model may be understood by an analogy to coin tossing. Consider an unbiased coin toss with outcome $P_n = \pm 1$ (analogous to the atmospheric forcing), and a sum $\sum P_n = X$ (analogous to the ocean response). In the absence of damping, the sum X will contain progressively longer time scales and fewer zero crossings as time increases (this is simply a random walk). As discussed below, damping limits the growth of variance for very long time scales. Standardized (idealized) time series of atmospheric forcing and oceanic temperature anomalies produced by the Hasselmann (1976) model are shown in Fig. 21. From this figure, it is clear that the model provides a means of producing low-frequency variability from a process with no preferred time scale.

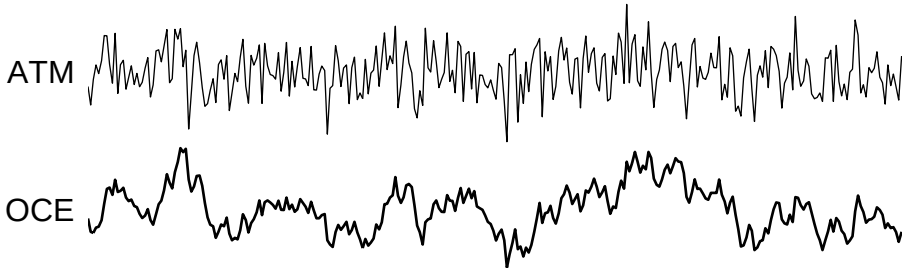

Fig. 21. Idealized standardized atmospheric forcing and oceanic response time series produced by the Hasselmann (1976) model.

The variance spectrum of ocean temperature anomalies may be written:

$$P_o(\omega) = \frac{f(\omega)}{\omega^2 + \lambda^2}, \qquad (2)$$

where $f(\omega)$ is the spectrum of atmospheric variability, which may be considered constant (white noise) for time scales longer than a week or so. For short time scales ($\omega >> \lambda$), the ocean temperature variance increases linearly with time, in accord with the random walk behavior discussed above. In the absence of the damping feedback, the ocean temperature anomaly would grow without bound. However, for these longer time scales, damping becomes progressively more important. As a result, for long time scales ($\omega << \lambda$), damping matches the increased variance from the integrative effect, and the spectrum flattens out. The spectrum produced by the Hasselmann (1976) model has been quite effective at describing the temporal variability of mid-latitude SST variability in numerous observational and modeling studies, and should be used as a null hypothesis for mid-latitude SST variability.

The Hasselmann (1976) model has been combined with a simple model of the reemergence mechanism (discussed in Section 4) by Deser et al. (2002) to successfully explain the year-to-year persistence of SST anomalies in the North Pacific. Shown in Fig. 22 is the auto-lag correlation of North Pacific SST and mixed layer heat content anomalies from their values in March. A clear annual cycle is seen in the SST autocorrelation (dashed line) with peaks in March of successive years, due to the reemergence mechanism. In contrast, the total heat content (which includes the contribution from temperature anomalies that are trapped at depth during the summer months) appears to decay at a constant rate, as expected by a theoretical Hasselmann (1976) model that uses the winter mixed layer depth to calculate the damping rate (thick grey line in Fig. 22). The success of this model implies that the *winter* mixed layer depth should be used when calculating the feedback parameter λ for studies of the year-to-year persistence of SST anomalies.

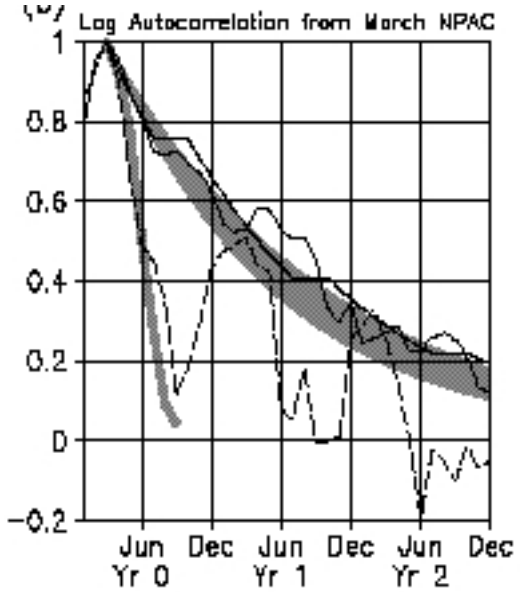

Fig. 22. Monthly lagged autocorrelation function from March for heat content (solid) and SST (dashed). The broad grey band indicates the theoretical spectrum from the idealized stochastic model of Deser et al. 2002. The thin grey line denotes the theoretical curve for the short term response of the Hasselmann (1976) model. From Deser et al. (2002).

One of the limitations of the Hasselmann (1976) model is that it does not allow for a coupled atmospheric response to ocean temperature anomalies. Barsugli and Battisti (1998) incorporate this response in a linear stochastic energy balance model of thermal coupling between the mid-latitude ocean and atmosphere. In contrast to Hasselmann (1976), intrinsic atmospheric dynamics are represented by a white noise process (*N*), heat flux anomalies are related to the sea-air temperature difference, and the atmosphere is permitted to respond to these heat flux anomalies. The resulting model may be written:

$$\frac{dT_a}{dt} = -aT_a + bT_o + N$$
$$\beta\frac{dT_o}{dt} = cT_a - dT_o \qquad (3)$$

where $-aT_a$ and $-dT_o$ represent damping of atmospheric and oceanic temperature anomalies; bT_o and cT_a represent ocean-to-atmosphere and atmosphere-to-ocean feedbacks, respectively; and β represents the ratio of thermal inertia between the ocean and atmosphere ($\beta >> 1$).

The power spectra of atmospheric and oceanic temperature anomalies from the coupled and uncoupled Barsugli and Battisti (1998) model (equation 2) are shown in Fig. 23, upper panel. Note that the uncoupled Hasselmann (1976) model may essentially be recovered from the Barsugli and Battisti (1998) model by setting b to zero, and noting that β introduces a disparity in the intrinsic time scales of atmospheric and oceanic variability such that T_a is essentially white at the time scales of interest to the ocean (see Fig. 23, uncoupled curves). Fig. 23, upper panel, shows that the addition of ocean-to-atmosphere feedbacks causes a three-fold increase in low-frequency (decadal) oceanic and atmospheric temperature variance. This increased variance results from a reduced thermal damping of temperature anomalies at low frequencies: as the oceanic and atmospheric temperature reach equilibrium, the net surface heat flux (proportional to the temperature difference) vanishes, reducing the thermal damping of both the ocean and atmosphere. This effect can be seen in the variance spectra of heat flux from the coupled and uncoupled experiments in Fig. 23, lower panel. The lack of appreciable heat flux anomalies at decadal time scales lends a cautionary note to the interpretation of surface heat fluxes as implying causality for decadal time scale fluctuations.

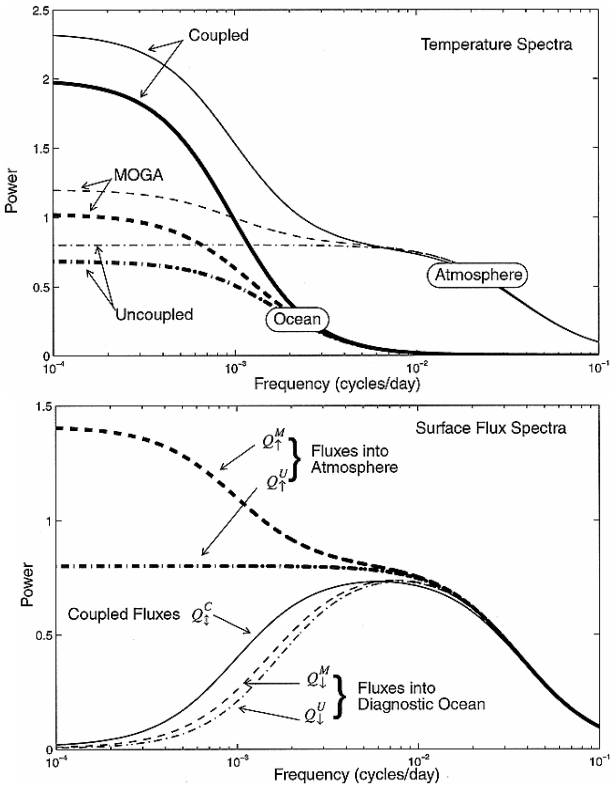

Fig. 23. Theoretical spectra from the Barsugli and Battisti (1998) model: (top) oceanic and atmospheric temperature spectra; (bottom) heat flux spectra. Coupled and uncoupled curves are discussed in text. From Barsugli and Battisti (1998).

The physical mechanism behind the Barsugli and Battisti (1998) model has been confirmed in GCM simulations. Bladé (1997, 1999), and Saravanan (1998) show that thermal coupling increases mid-latitude 500mb height variance by about 20%, and increases 850mb temperature variance by about 70%. These studies confirm that thermal coupling decreases the net surface heat flux variance, resulting in a positive feedback for atmospheric temperature anomalies. Blade (1999) shows that thermal coupling tends to enhance the variance of "zonal index" modes (such as the WP and NPO patterns) more so than other modes (e.g., the PNA).

The inclusion of a dynamic ocean introduces new mechanisms by which a defined decadal time scale might be generated (Frankignoul et al., 1997; Saravanan and McWilliams 1998; Weng and Neelin, 1999). In these hypotheses, a time scale is set by a defined spatial scale of atmospheric forcing, and an advective velocity set by ocean processes. Consider, in the case of Frankignoul et al. (1997), a spatially uniform but temporally stochastic wind stress curl that forces baroclinic oceanic Rossby waves. As the Rossby waves propagate westward, they integrate the wind stress curl forcing, producing a maximum streamfunction response at the western boundary of the ocean basin. The dominant time scale of that response is thus set by the basin width (or spatial scale of the atmospheric forcing) and the advective velocity of the first baroclinic Rossby wave.

The advective resonance hypothesis of Saravanan and McWilliams (1998), illustrated in Fig. 24 below, may be understood in a similar fashion, except that the ocean integrates heat flux forcing with a defined spatial scale along a trajectory determined by the mean gyre circulation (and hence a defined advective velocity). Note that both the Frankignoul et al. (1997) and Saravanan and McWilliams (1998) mechanisms produce defined decadal time scale variability without any requirement of atmospheric feedbacks. Naturally, the spectra might be altered if a Barsugli and Battisti (1998) feedback is incorporated into the atmospheric forcing.

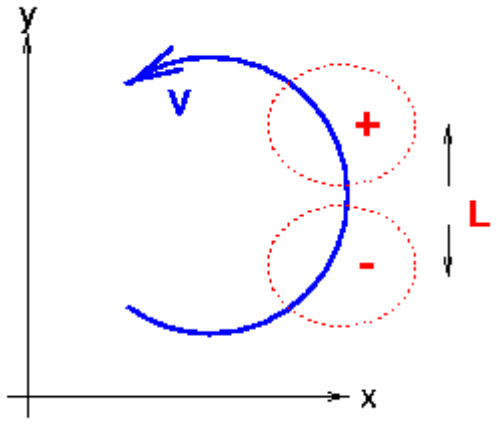

Fig. 24. Schematic of the advective resonance hypothesis of Saravanan and McWilliams (1998). Arrows denote mean gyre circulation, lightly dashed lines indicate fixed pattern of atmospheric forcing. From Saravanan et al. (2000).

Various studies have investigated the hypotheses of Frankignoul et al. (1997) and Saravanan and McWilliams (1998) in model simulations. The modeling studies of Frankignoul et al. (2000) and Schneider et al. (2002) find that the mid-latitude Pacific Ocean response to atmospheric forcing includes both a quick response to surface fluxes and Ekman advection, and a delayed response along the western boundary arising from the oceanic adjustment to wind stress curl forcing (as per Frankignoul et al., 1997). In contrast, Pierce et al. (2001) investigates the role of ocean dynamics in producing mid-latitude decadal variability, and finds that neither the advective resonance hypothesis of Saravanan and McWilliams (1998), nor the stochastic excitation of oceanic Rossby waves can explain a modeled decadal peak in the variance spectrum of oceanic variability.

5.2.2. Uncoupled mechanisms

It is possible that decadal variability may be generated in the atmosphere or ocean without any coupling between the two. It is possible that chaotic attractors in the atmosphere may give rise to preferred 'regimes' of atmospheric variability. External forcing by increased carbon dioxide may bias the atmosphere toward one regime over another. This behavior is suggested by the results of Corti et al. (1999), shown in Fig. 25. They show that the atmospheric state probability density function (PDF), based on the 500mb geopotential height field, has undergone a change in the early 1970's, which may be due to greenhouse gas forcing. Internally generated ocean variability may also give rise to decadal variability. In the Atlantic, interactions between the ocean's gyre and thermohaline circulations may give rise to variability with a decadal time scale. Though quite weak, it is possible that this effect may be rapidly (~40 yr) communicated to the tropical Pacific through wave dynamics (Goodman, 2000). Other studies of eddy-resolving ocean models (see Miller and Schneider, 2000 for a review) indicate that decadal variability may arise independent of atmospheric forcing. Despite the existence of uncoupled mechanisms in the atmosphere and ocean, it is unlikely that decadal variability of appreciable amplitude can be generated in the absence of coupling, except possibly in the Kuroshio region.

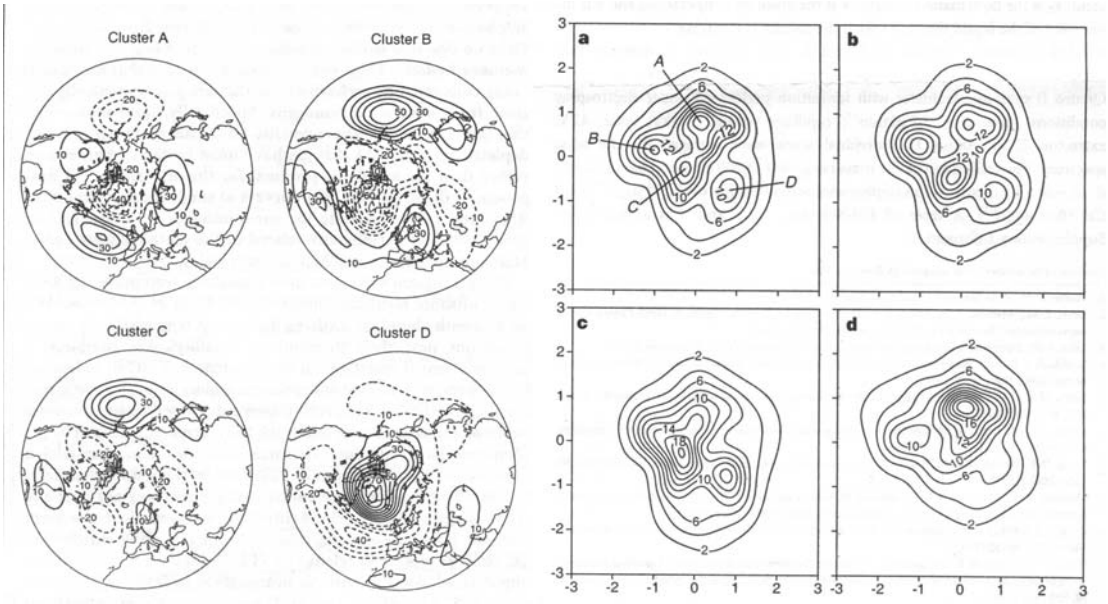

Fig. 25. Left panels: preferred regimes of atmospheric variability, obtained by cluster analysis. Right panel: 500mb geopotential height state vector PDF expressed as a projection onto the first two EOFs of monthly mean 500mb height. Panel (a) indicates the location of the clusters (left panels) in the state space. Panel (c) indicates the PDF for the time period 1949-1971, and panel (d) indicates the PDF for the time period 1971-1994. From Corti et al., (1999).

5.2.3 Mid-latitude coupled modes

Coupled feedbacks between the mid-latitude ocean and atmosphere may give rise to new intrinsic mid-latitude modes of decadal variability (Latif and Barnett 1994, 1996; Weng and Neelin, 1999). One such mode is hypothesized by Latif and Barnett (1994) in a 70 year simulation of the ECHO coupled model. The mode is described in the following manner. Suppose an anomalous atmospheric circulation cools the central Pacific SST through changes in the net surface heat fluxes and Ekman transports. If this SST anomaly feeds back positively to the atmospheric circulation anomaly, it will tend to add persistence to the atmospheric circulation anomalies. At the same time, wind stress anomalies associated with the atmospheric circulation strengthen the subtropical gyre circulation, which advects warmer water northward along the western boundary, and into the KOE region. The resulting warm SST anomalies feed back negatively to the atmospheric circulation and switches the phase of the oscillation.

The Latif and Barnett (1994, 1996) mechanism has been extensively investigated in various coupled and uncoupled model simulations. The mid-latitude ocean response to observed atmospheric forcing is examined in Miller et al. (1994, 1998) and Seager et al. (2001). The oceanic response in the KOE region consists of a fast response to local surface forcing (as per the Hasselmann, 1976 mechanism), and

a delayed dynamical response of the thermocline in the KOE region, due to Rossby wave propagation from the central Pacific. This thermocline response is communicated to the surface by mixed layer processes during the winter. However, both models (those mentioned, as well as Schneider et al. 2001; Frankingnoul et al. 2002) and observations (Deser et al., 1999), suggest that the resulting SST anomalies in the KOE region are the wrong sign to force a negative feedback, as per the Latif and Barnett (1994, 1996) mechanism. The atmospheric response to mid-latitude SST anomalies has also been studied extensively in modeling simulations. In general, it is found that the modeled response to mid-latitude SST anomalies is much weaker than that in the ECHO model simulation used by Latif and Barnett (1994) (see Kushnir et al. 2002, for a review).

While it does not appear that the Latif and Barnett (1994) mechanism, in its original state is likely to explain observed decadal variability, feedbacks from the ocean to the atmosphere do appear to play some role in generating variability in some GCM simulations. In particular, the coupled model simulations of Frankignoul et al. (2002) and Schneider et al. (2002) both suggest a weak positive feedback between ocean SST anomalies in the KOE region and the overlying atmospheric circulation. Shown in Fig. 26 is the spectrum of ocean pressure near the KOE region from a 147yr simulation of the ECHO-2 model (an improved version of the same model used by Latif and Barnett (1994)), as well as the expected spectra from some theoretical models. In the left panel, the modeled spectrum compares very well with a simple equivalent barotropic Rossby wave model that is forced by the coupled model's wind stress curl field. The middle panel shows the spectrum that would be expected if the atmospheric forcing were purely a white-noise process (i.e., without feedbacks from the ocean to the atmosphere). The agreement between the simple model and the GCM in the middle panel suggest that pressure variability in the western Pacific is largely governed by the Frankignoul et al. (1997) mechanism. In the right panel, the GCM spectrum is compared to the same Rossby wave model, except that the model includes either a negative (as per Latif and Barnett, 1994) or a positive feedback. While the negative feedback does produce a weak spectral peak, it is at too short a period, and the interdecadal variance is too weak to explain the ECHO-2 model's variability. Instead, a weak positive feedback may be important for the model's variability.

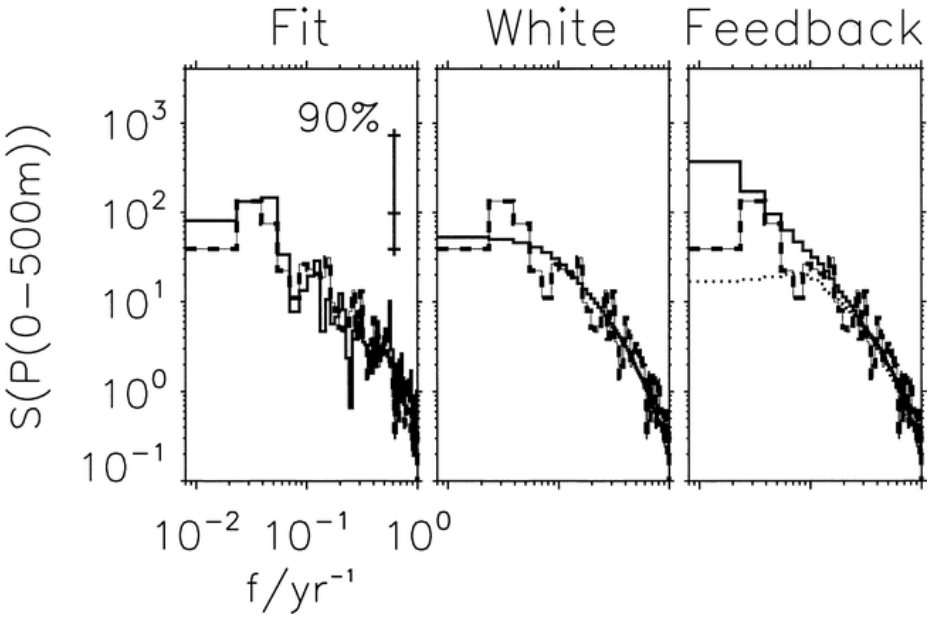

Fig. 26: Ocean pressure spectra from the ECHO-2 model (from Schneider et al. 2002): (left panel) CGCM ocean pressure spectrum (dashed) compared to the spectrum produced by a simple equivalent barotropic Rossby wave model (solid); (middle panel) CGCM spectrum (dashed) compared to the same Rossby wave model, with white noise atmospheric forcing. (right panel); model spectrum compared to the same Rossby wave model that incorporates a positive (solid) or negative (dotted) feedback.

5.3 Connections between the tropics and mid-latitudes

In this section we present some hypotheses through which the mid-latitudes and tropics interact with one another. First, we present the well-established "atmospheric bridge" null hypothesis, which is known to operate on interannual time scales. Next, connections by which the mid-latitudes influence the tropics through oceanic processes are presented, followed by a mechanism by which the mid-latitude atmosphere can influence the tropics through coupling with the oceanic mixed layer in the tropics and subtropics.

5.3.1 The atmospheric bridge

It is well established that tropical ENSO variability forces mid-latitude atmospheric teleconnections, which may then force temperature anomalies in the underlying ocean (see reviews by Lau, 1997; Trenberth et al., 1998; Alexander et al., 2002). Although there is still some controversy about the details of the mid-latitude teleconnections, it is generally accepted that ENSO-related changes in the tropical circulation (due to changes in tropical atmospheric heating) provide a forcing mechanism for poleward propagating Rossby waves in the atmosphere. Due to climatological features in the mid-latitude atmosphere, the atmospheric response

typically takes on features of existing modes of atmospheric variability. This atmospheric variability can, in turn, alter the mid-latitude SST through associated changes in the surface heat and momentum fluxes. The prevalence of the atmospheric bridge on interannual time scales, combined with the assumed existence of tropical ENSO-related decadal variability, suggests that the atmospheric bridge should be used as a null hypothesis for explaining interactions between the tropics and mid-latitudes on decadal time scales.

Modeling studies have confirmed the role of tropical ENSO-like variability in reproducing observed mid-latitude climate variability. Graham (1994) and Graham et al. (1994) perform a series of model simulations in which an atmospheric model is forced by observed tropical (TOGA), mid-latitude (MOGA) and global (GOGA) SSTs. They find that many elements of the 1976-77 shift in mid-latitude climate are reproducible when the atmosphere is forced by tropical SST anomalies, in accord with the atmospheric bridge hypothesis.

5.3.2 Connections involving ocean transports

Numerous mechanisms have been proposed by which mid-latitude variability impacts tropical ENSO-like variability through oceanic pathways. Gu and Philander (1997) propose a decadal cycle by which mid-latitude SST anomalies (generated through the atmospheric bridge) subduct at mid-latitudes and propagate westward and equatorward through the ocean's interior. Upon reaching the equator, these cool temperature anomalies encounter temperature anomalies of the opposite sign, eventually reversing the sign of the tropical temperature anomalies, and hence the decadal SST anomalies.

Though the Gu and Philander mechanism may exist in some simple coupled models, recent research indicates that it is not likely to have an important effect in models or in nature (Schneider, 1999; Pierce et al., 2000; Liu et al., 2002). Kleeman et al. (1999) propose a similar mechanism by which teleconnected mid-latitude wind stress anomalies alter the strength of the subtropical overturning cells, eventually affecting the equatorial SST. Some evidence for a spin-down of the subtropical gyre circulation is presented by McPhaden and Zhang (2002), although it is unclear whether this spin-down is forced by mid-latitude variability, or by tropical coupled dynamics. Lysne et al. (1997) propose a similar mechanism by which Rossby waves generated by teleconnected wind stress anomalies may reflect off the western boundary, eventually affecting the tropical thermocline.

5.3.3 Connections involving the atmosphere

It is possible that intrinsic mid-latitude atmospheric variability may influence the tropics through coupled interactions with the tropical Pacific mixed layer. Vimont et al. (2001) outline a "seasonal footprinting mechanism" (SFM) that

links mid-latitude atmospheric variability with tropical zonal wind stress anomalies, which may subsequently influence ENSO. The mechanism is summarized in Fig. 27. During winter, mid-latitude atmospheric variability with a spatial structure that closely resembles the NPO of Walker and Bliss (1932), imparts an SST "footprint" onto the oceanic mixed layer via changes in the net surface heat flux. The subtropical portion of this footprint persists into the spring and summer, and forces a residual atmospheric circulation that includes zonal wind stress anomalies along the equator. The tropical Pacific responds to these equatorial zonal wind stress anomalies through coupled dynamics, producing an ENSO-like pattern of variability.

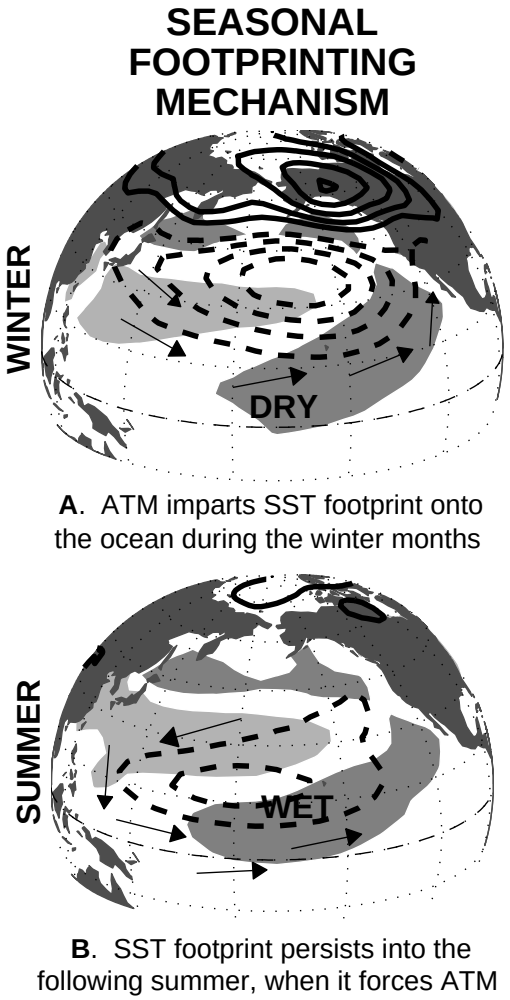

A. ATM imparts SST footprint onto the ocean during the winter months

B. SST footprint persists into the following summer, when it forces ATM

Fig. 27. Schematic of the Seasonal Footprinting Mechanism. Dashed lines indicate SLP anomalies, arrows denote surface winds, and dark and light shading indicate warm and cold SST anomalies, respectively. From Vimont et al. (2002b).

The SFM appears to play an important role in generating tropical variability in nature, and in the CSIRO models. Vimont et al. (2002a) find that the SFM explains 25-50% of the CSIRO model's interannual ENSO variability, and nearly 75% of the model's decadal ENSO-like variability. In the observed record, Vimont

et al. (2002b) find the SFM may be a leading contributor to the stochastic forcing of ENSO. Fig. 28 shows the temporal evolution and lagged correlation between indices of the NPO and of ENSO, from Vimont et al. (2002b). Indeed, the lagged correlation confirms that the winter NPO tends to lead to an ENSO event during the following winter. Although Vimont et al. (2002b) focused on the relationship between the NPO and interannual ENSO variability, examination of Fig. 28 suggests that the SFM may play a role in generating decadal variability in nature as well.

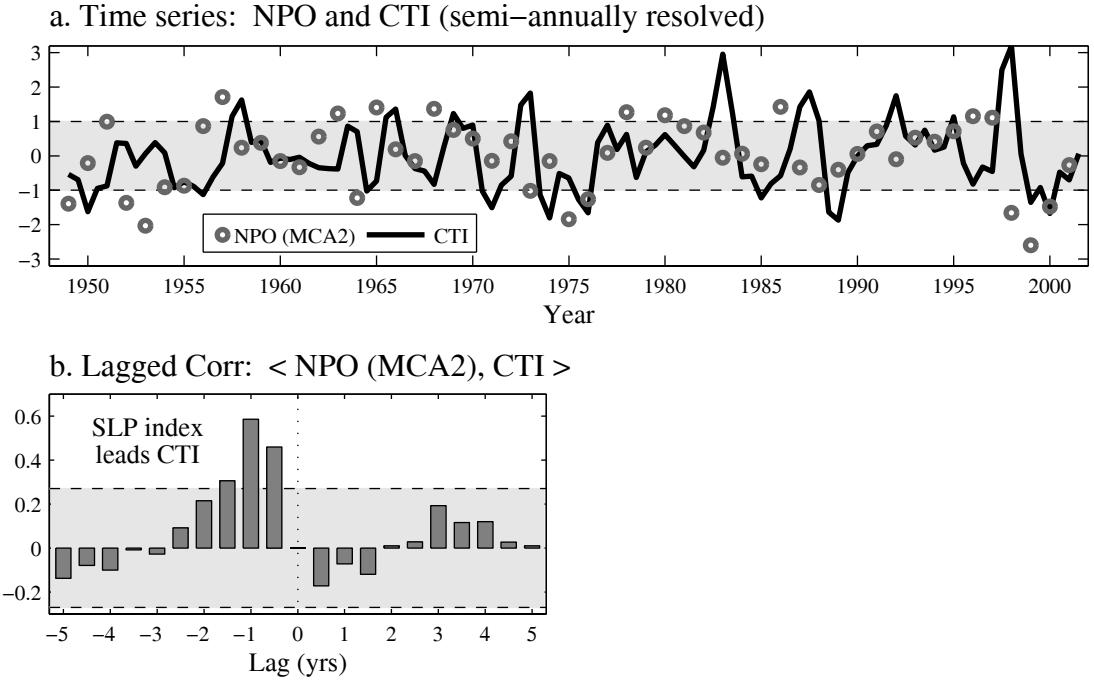

Fig. 28. (a) Time series of the observed, semi-annually resolved CT index (solid line), and of a time index representing the winter NPO (grey circles). (b) Lagged correlation between the NPO time series and the CT index in part (a). For reference, in panel (b), a lag of -1/2 (-1) implies that the winter NPO leads the following summer (winter) CTI. From Vimont et al. (2002c).

6. Where Are We, and Where Do We Go From Here?

6.1. Mechanisms

There appears to be a growing consensus on the mechanisms responsible for the bulk of the decadal variability in the Pacific. This consensus has been aided by the emergence of viable and testable null hypotheses for decadal variability. Here, we present a brief collection of null hypotheses that appear to be important for explaining the low-frequency (decadal) variability in the Pacific. While not

exhaustive, these hypotheses should be considered before resorting to more "exotic" mechanisms for describing decadal variability.

From models, it is well established that ENSO varies on many time scales, including decadal. This tropical decadal variability arises simply from the ENSO cycle itself. Modeling results indicate that stochastic forcing may play a very important role in determining the strength and temporal characteristics of tropical decadal variability. In particular, the mid-latitude atmosphere (through the seasonal footprinting mechanism) may be an important source of tropical decadal variability.

The mid-latitudes will be affected by decadal ENSO variability through the Atmospheric Bridge. However, tropically forced mid-latitude decadal variability is only half the story (the correlation between the CTI and the PDO is only about 0.7) – there is still a good deal of variability that arises due to processes intrinsic to the mid-latitudes. Intrinsic mid-latitude decadal variability appears mainly driven by two mechanisms:

1) The bulk of the SST variability may be considered as a broad-scale, immediate response to local surface forcing from the atmosphere (either intrinsic, or tropically forced) as in the Hasselmann (1976) and Barsugli and Battisti (1998) mechanisms. These SST anomalies persist from year to year due to the reemergence mechanism, as shown by Deser et al., 2002.

2) A delayed, non-local response to atmospheric forcing is generated through ocean dynamic processes. This response is produced by westward propagating Rossby waves, and hence is strongest at the western boundary of the ocean basin (Frankignoul et al., 1997). An SST signature of this non-local response may be induced through changes in the strength of the gyre circulation, shifts in the location of the Kuroshio, and displacements of the mid-latitude thermocline which affect the surface by deep mixing during the winter. The effects of these temperature anomalies on the overlying atmospheric circulation are weak, though perhaps not trivial. The role of uncoupled ocean processes may also prove important in explaining variability of in the Kuroshio region.

It appears that midlatitude SST anomalies have only a small and subtle effect on the atmosphere (e.g. Kushnir et. al, 2002) and it is most likely that the SST anomalies in midlatitudes independent of SST do not directly force midlatitude teleconnections. This is especially important when considering impacts and predictability of decadal variability. In particular, while simultaneous correlations such as Fig. 1 indicate large impacts of decadal variability over the northwestern

U.S., it is most likely that any predictable component of these impacts will come from the tropics (Pierce, 2002).

The role of seasonality has been highlighted by Deser et al. (2001), Barlow et al. (2001), and by Vimont et al. (2001, 2002b, 2002c). It seems that any theory of decadal variability must also deal with the issue of seasonality.

The local response to surface forcing is illustrated in Fig. 29, which is generated from a coupled simulation of an atmospheric GCM coupled to an ocean slab mixed layer (a similar result was obtained by Barnett et al., 1999a and Pierce et al, 2000). Clearly visible in Fig. 29 is an SST anomaly at 40ºN that must have been forced from the atmosphere since there is no other process that can create SST anomalies in a mixed layer ocean-in particular there is no Kuroshio. At the same time modeling studies that include a dynamic ocean have indicated that similar low-frequency variability near the Kuroshio region can arise through displacements of the Kuroshio (Deser, personal communication). That it is an ocean process in this model is unambiguously decided by finding that the fluxes connected to this SST are opposed to the SST anomaly and therefore could not have been the cause of it. This non-local effect is likely to be spatially attenuated by the ocean.

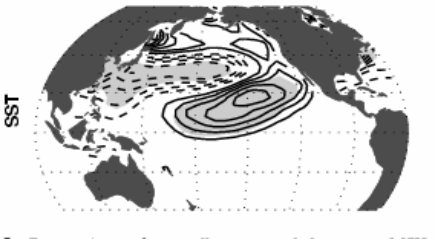

Fig 29: SST from an AGCM coupled to a slab ocean mixed layer. From Vimont et al, 2002b.

6.2. Observations

Its clear that the observational record is too short to completely define decadal variability. SST is known partly for the last 120 years and reconstructions (Kaplan et al., 1998) have (arguably) allowed a complete SST field of the Pacific for the this interval. The COADS data set usefully allows construction of the subsidiary fluxes for only about the last 50 years. Similarly for the upper air structure, data exists only for the last 50 years and no amount of reanalysis can provide data where none was ever taken. It therefore becomes a challenge to extract decadal and multi-decadal signals from the observations.

The record *is* long enough to identify some decadal variability and this is what we have reviewed in Section 2. Still, one cannot help but question whether the dominant methods (EOF analysis and temporal filtering) are appropriate for identifying decadal variations. A glance at the movie of SSTs since 1980 at http://www.coaps.fsu.edu/~grant/reysst makes the problem clear. The patterns

identified by the EOF analyses in Sec. 2 don't individually last for decades but they sometimes do appear in full form for brief periods. More often, however, pieces of them recur often enough for the EOF analysis to put them together as a pattern.

It should also be noted that the subsurface structure is not well enough defined by the observations to examine the full three dimensional structure in the ocean of the patterns identified in Sec. 2. Thus while models have been used to drive the subsurface structure using the observed winds (e.g. Miller et al., 1994, 1998; Xie et al., 2000; Seager et al., 2001; Karspeck and Cane, 2002; Giese and Carton, 1999), these are not subject to observational verification (except near the equator) since the mid 1990s.

The record has been extended by used of paleoclimatic proxies. As an example, Minobe (1997) uses a tree ring reconstruction to identify a time scale for Pacific decadal variability of order 50-70 years. The observational record is too short to confirm the prevalence of this time scale although Tanimoto et al., 1994 and later authors have certainly tried. The use of tree rings as proxies is actively being explored to extend the record still further (e.g. Biondi et al., 1991; Gedalof et al., 2001).

We should be doing everything in our power to guarantee that in one hundred years, we have extended the observational record in the Pacific by one hundred years and that we have the data needed to define the decadal variability. If things proceed as at present, this will not be true. At the same time, we need to work to extend the temporal and spatial coverage of paleoclimatic data while we can (e.g. records from tropical glaciers and corals are being lost as the earth warms due to anthropogenic emissions).

6.3. Models

Regardless of the quality of observational record, in the near future the data record will simply be too short to unambiguously determine the mechanisms responsible for Pacific decadal variability, especially given the prevalence of stochastic processes. Additionally, the increase of greenhouse gasses will make it increasingly more difficult to distinguish natural climate variability from externally forced climate variability. Thus, the laboratory that models provide will be essential for distilling the physics responsible for decadal variability in the climate system. The unraveling of mechanisms are therefore most likely to be accomplished in climate models guided by whatever observations exist.

This is not to downplay the importance of observational studies. It should be noted that every theory of decadal variability involves physical processes that occur on much shorter time scales – from days to years. The data record is clearly long enough to examine these short time scale processes, and hence, to provide some

limits on the validity of proposed theories of decadal variability. Similarly, observational studies will continue to provide estimates of the range and structure of decadal variability in nature.

One area that should be focused on is the improvement of coupled climate models, especially in representing tropical variability, and in representing the boundary currents. Currently, there are no GCMs that produce a realistic ENSO cycle (with respect to amplitude, irregularity, phase locking to the seasonal cycle, etc.). This is of utmost importance in understanding not only decadal variability, but also the mean climate, the sensitivity of climate, the climate response to increased greenhouse gasses, and the variability and mean state of past climates. A realistic representation of the western boundary currents will be important in determining predictability limits along the western boundary (as shown in Schneider and Miller, 2001), and the potential atmospheric feedbacks to ocean heat flux anomalies.

As we have pointed out, much of the knowledge about the mechanisms of Pacific decadal variability is likely to be obtained from the analysis of climate models. Thus, a detailed intercomparison of the decadal variability in climate models would be of value. This having been done, a complete diagnostic analysis of known mechanisms for decadal variability (as outlined in Section 6.1) in each of them would be of immense value for exploring the range of possible mechanisms for pacific decadal variability. Once these mechanisms have been explored, it is worth asking whether any of the models derive Pacific decadal variability from anything other than the null hypothesis combined with the decadal variability of ENSO.

Acknowledgements: This work was supported by a grant from the NOAA Office of Global Programs to the Center for Science in the Earth System. We are indebted to Clara Deser for valuable discussions.

7. References

a. General References on Decadal Variability

Anderson D.L.T., and J. Willebrand, eds., 1996: *Decadal Climate Variability: Dynamics and Predictability*. NATO ASI Series Vol. 144, Springer-Verlag, 493pp.

Higgins, R. W., A. Leetmaa, Y. Xue, and A. Barnston, 2000: Dominant factors influencing the seasonal predictability of U.S. precipitation and surface air temperature. *Journal of Climate,* **13**, 3994–4017.

Mantua, N.J., and S.R. Hare, 2001: The Pacific Decadal Oscillation. *J. Oceanography* (Japan), **58**, 35-44.

National Research Council, 1995: *Natural Climate Variability on Decade-to-Century Time Scales.* National Academy Press, 630 pp. (Available for reading at www.nap.edu).

National Research Council, 1998: *Decade-to-Century-Scale Climate Variability and Change. A Science Strategy*. National Academy Press, 142pp.
(Available for reading at www.nap.edu).

Sarachik, E.S., M. Winton, and F.-L. Yin,: Mechanisms for decadal-to-centennial climate variability. In *Decadal Climate Variability: Dynamics and Predictability*. NATO ASI Series Vol. 144, Springer-Verlag, pp 157-210.

WCRP, 1995: CLIVAR Science Plan. WCRP-89, WMO/TD 690, 157 pp.

WCRP, 1998: CLIVAR Initial Implementation Plan, WMO/TD 869, 314pp + Appendices. Especially Sec III.8: Pacific and Indian Ocean Decadal Variability, pp 231-258.

2. Pacific Decadal Variability: Observations

Alexander, M. A., and C. Deser, 1995: A mechanism for the recurrence of wintertime midlatitude SST anomalies. *J. Phys. Oceanogr.*, **25,**122-137.

Alexander, M. A., M. S. Timlin, and J. D. Scott, 2001: Winter-to-winter recurrence of sea surface temperature, salinity and mixed layer depth anomalies. *Prog. Oceanography,* **49***,* 41-61.

Alexander, M. A., C. Deser, and M. S. Timlin, 1999: The reemergence of SST anomalies in the North Pacific Ocean. *J. Climate*, **12,** 2419-2433

Barnston A. G., and R. E. Livezey, 1987: Classification, seasonality and persistence of low-frequency atmospheric circulation patterns. *Mon. Wea. Rev.*, **115**, 1083-1126.

Barlow, M., S. Nigam, and E. H. Berbery, 2001: ENSO, Pacific Decadal Variability, and U.S. Summertime Precipitation, Drought, and Stream Flow. *J. Climate,* **14**, 2105–2128.

Biondi, F., A. Gershunov, and D.R. Cayan, 2001: North Pacific decadal climate variability since 1661. *J. Climat*e, **14**, 5-10.

Blackmon, M. L., Y.-H. Lee and J. M. Wallace, 1984: Horizontal Structure of 500 mb Height Fluctuations with Long, Intermediate and Short Time Scales *J. Atmos. Sci*. **41**, 961–980.

Bond, N.A. and D.E. Harrison, 2000: The Pacific Decadal Oscillation, air-sea interaction and central north Pacific winter atmospheric regimes. *Geophys. Res. Lett.*, **27**, 731-734.

Cheng, X., G. Nitche, and J.M. Wallace, 1995: Robustness of low-frequency circulation patterns derived from EOF and rotated EOF analyses. *J. Climate,* **8**, 1709-1713.

Deser, C., and M. L. Blackmon, 1995: On the relationship between tropical and North Pacific sea surface temperature variations. *J. Climate,* **8,** 1677–1680.

Deser, C., M. A. Alexander, and M. S. Timlin, 1996: Upper-ocean thermal variations in the North Pacific during 1970–1991. *J. Climate,* **9**, 1840–1855.

Deser, C., M.A. Alexander, and M.S. Timlin, 1999: Evidence for a wind-driven intensification of the Kuroshio Current Extension from the 1970s to the 1980s. *J. Climate*, **12**, 1697-1706.

Deser, C., M.A. Alexander, and M.S. Timlin, 1996: Upper ocean thermal variations in the North Pacific during 1970-1991. *J. Climate*, **9,** 1840-1855.

Deser, C., and M.S. Timlin (1997): Atmosphere-ocean interactions on weekly timescales in the North Atlantic and Pacific. *J. Climate,* **10**, 393-408.

Dettinger, M.D., D.S. Battisti, R.D. Garreaud, G.J. McCabe Jr., and C.M. Bitz, 2000: Interhemispheric effects of interannual and decadal ENSO-like climate variations on the Americas. In *Present and Past Interhemispheric Climate Linkages in the Americas and their Societal Effect*s. Ed. by V. Markgraf, Cambridge University Press. Cambridge, UK, p. 1-16.

Enfield, D.B., and A.M. Mestas-Nuñez, 2000: Interannual to multidecadal climate variability and its relationship to global sea surface temperature. In *Present and Past Interhemispheric Climate Linkages in the Americas and their Societal Effect*s. Ed. by V. Markgraf, Cambridge University Press. Cambridge, UK, p17-29.

Folland, C.K., and D.E. Parker, 1990: Observed variations of sea surface temperature. In *Climate-Ocean Interactions*, M.E. Schlesinger, editor, Kluwer Publishers.

Folland, C.K., and D.E. Parker, 1995: Correction of instrumental biases in historical sea surface temperature data. *Q. J. Roy. Met. Soc.*, **121**, 319-367.

Garreaud, R.D. and D.S. Battisti, 1999: Interannual ENSO and interdecadal ENSO-like variability in the Southern Hemisphere tropospheric circulation. *J. Climat*e, **12**, 2113-2123.

Gedalof, Z. and D. J. Smith, 2001: Interdecadal climate variability and regime-scale shifts in Pacific North America. *Geophys. Res. Lett.*, **28**, 1515-1518.

Gershunov, A. and T. P. Barnett, 1999: Interdecadal modulation of ENSO teleconnections. *Bull. Amer. Meteor. Soc.,* **79**, 2715-2725.

Giese, B.S., and J.A. Carton, 1999: Interannual and decadal variability in the tropical and mid-latitude Pacific Ocean. *J. Climate*, **12**, 3402-3418.

Guilderson, T.P., and D.P. Schrag, 1998: Abrupt shift in subsurface temperature in the tropical Pacific associated with changes in El Niño. *Science*, **281**, 240-243.

Halpert, M. S., and C. F. Ropelewski, 1992: Surface temperature patterns associated with the Southern Oscillation. *J. Climate,* **5,** 577–593.

Hamlet, A.F., and D.P. Lettenmaier, 1999: Columbia River Streamflow Forecasting Based on ENSO and PDO Climate Signals, *ASCE J. of Water Res. Planning and Mgmt.,* **125**, 333-341.

Hare, S. R., and N. J. Mantua, 2000: Empirical evidence for North Pacific regime shifts in 1977 and 1989, *Prog. Oceanography*, **47,** *103-145.*

Harrison, D.E. and N.K. Larkin, 1998: El Nino-Southern Oscillation surface temperature and wind anomalies, 1946-1993. *Revs. Geophys.*, **36**, 353-399.

Horel, J. D., and J. M. Wallace, 1981: Planetary-scale atmospheric phenomena associated with the Southern Oscillation. *Mon. Wea. Rev.,* **109**, 813–829.

Hsu, H.-H., and J.M. Wallace, 1985: Vertical structure of wintertime teleconnection patterns. *J. Atmos. Sci.*, **42**, 1693-1710.

Hurrell, J.W., 1996: Influence of variations in extratropical wintertime teleconnections on Northern Hemisphere temperatures. *Geophys. Res. Lett.*, **23**, 665-1996.

Kachi, M., and T. Nitta, 1997: Decadal variations of the global atmosphere-ocean system. *J. Meteor. Soc. Japan,* **75**, 657–675.

Kalnay, E., M. Kanamitsu, R. Kistler, W. Collins, D. Deaven, L. Gandin, M. Iredell, S. Saha, G. White, J. Woollen, Y. Zhu, A. Leetmaa, R. Reynolds, M. Chelliah, W. Ebisuzaki, W.Higgins, J. Janowiak, K. C. Mo, C. Ropelewski, J. Wang, R.Jenne, D.Joseph, 1996: The NCEP/NCAR 40-Year Reanalysis Project. *Bull.. Am. Met. Soc.*, **77**, 437-472.

Kaplan, A., M. Cane, Y. Kushnir, A. C. Clement, M. B. Blumenthal, and B. Rajagopalan, 1998. Analyses of global sea surface temperature 1856-1991. *J. Geophys. Res.*,**103**, 18,567-18,589.

Kawamura, R., 1994: A rotated EOF analysis of global sea surface temperature variability with interannual and interdecadal scales. *J. Phys. Oceanogr.,* **24,** 707–715.

Kushnir, Y., and J. M. Wallace, 1989: Low-Frequency Variability in the Northern Hemisphere Winter: Geographical Distribution, Structure and Time-Scale Dependence. *J. Atmos. Sci.,* **46**, 3122-3143.

Lau, N.-C., 1997: Interactions between global SST anomalies and the midlatitude atmospheric circulation. *Bull. Amer. Meteor.Soc.,* **78**, 21-33.

Mantua, J. N., S. R. Hare, Y. Zhang, J. M. Wallace, and R. C. Francis, 1997: A Pacific interdecadal climate oscillation with impacts on salmon production. *Bull. Amer. Meteor. Soc.,* **78**, 1069-1080.

McPhaden, M. J., and D. Zhang, 2002: Slowdown of the meridional overturning circulation in the upper Pacific Ocean. *Nature*, **415**, 603-608.

Miller, A.J., D.R. Cayan, T.P. Barnett, N.E. Graham, and J.M. Oberhuber, 1994: The 1976-77 climate shift of the Pacific Ocean. *Oceanography*, **7**, 21-26.

Minobe, S., 1997: A 50–70-year climatic oscillation over the North Pacific and North America. *Geophys. Res. Lett.,* **24**, 683–686.

Minobe, S., 2000: Spatio-temporal structure of the pentadecadal variability over the North Pacific *Prog. Oceanogr.* **47**, 381–408

Nakamura, H., 1996: Year-to-year and interdecadal variability in the activity of intraseasonal fluctuations in the Northern Hemisphere wintertime circulation. *Theor. Appl. Climatol.,* **55**, 19–32.

Nakamura, H., G. Lin, and T. Yamagata, 1997: Decadal climate variability in the north pacific during the recent decades. *Bull. . Am. Met. Soc.,* **78**, 2215–2225.

Nitta, T., and S. Yamada, 1989: Recent warming of tropical sea surface temperature and its relationship to the Northern Hemisphere circulation. *J. Meteor. Soc. Japan,* **67**, 375–382.

Nitta, T., and M. Kachi, 1994: Interdecadal variations of precipitation over the tropical Pacific and Indian Oceans. *J. Meteor. Soc. Japan,* **72**, 823–831.

Norris J. R., Zhang, Y., and J. M. Wallace, 1998: Role of low clouds in summertime atmosphere–ocean interactions over the North Pacific. *J. Climate,* **11**, 2482–2490.

Schneider, N, A. J. Miller, 2001: Predicting Western North Pacific Ocean Climate. *J. Climate*: **14**, 3997–4002

Schubert, S.D., 1986: The structure, energetics, and evolution of the dominant frequency-dependent modes. *J. Atmos. Sci.*, **43**, 1210-1237.

Schwing, F. B., T. Murphree and P. M. Green, 2002: The Northern Oscillation Index (NOI): a new climate index for the northeast Pacific**,** *Prog. Oceanogr.,* **53**, 115-139.

Tanimoto, Y., N. Iwasaka, K. Hanawa, and Y. Toba, 1993: Characteristic variations of sea surface temperature with multiple time scales on the North Pacific. *J. Climate,* **6,** 1153–1160.

Tourre, Y. M., Y. Kushnir, and W. B. White, 1999: Evolution of interdecadal variability in sea level pressure, sea surface temperature, and upper ocean temperature over the Pacific Ocean. *J. Phys. Oceanogr.,* **29**,1528–1541.

Tourre, Y. M., B. Rajagopalan, Y. Kushnir, M. Barlow, and W.B. White, 2001: Patterns of coherent decadal and interdecadal climate signals in the Pacific Basin during the 20th Century. *Geophys. Res. Lett.*, **28**, 2069-2072.

Trenberth, K. E., 1990: Recent observed interdecadal climate changes in the Northern Hemisphere. *Bull. Amer. Meteor. Soc.,* **71**, 988–993.

Trenberth, K. E., and J. W. Hurrell, 1994: Decadal atmosphere-ocean variations in the Pacific. *Climate Dyn.,* **9**, 303–319.

Vimont, D. J., J. M. Wallace, and D. S. Battisti, 2002c: The seasonal footprinting mechanism in the CSIRO general circulation models. *J. Climate*, Submitted.

Walker, G. T., and E. W. Bliss, 1932: World weather V. *Mem. Roy. Meteor. Soc.*, 29-64.

Wallace, J. M., and D. S. Gutzler, 1981: Teleconnections in geopotential height field during the Northern Hemisphere winter. *Mon. Wea. Rev.,* **109**, 784–812.

Wallace, J. M., Y. Zhang, and K.-H. Lau, 1993: Structure and seasonality of interannual and interdecadal variability of geopotential height and temperature fields in the Northern Hemisphere troposphere. *J. Climate,* **6**, 2063–2082.

Wallace, J. M., Y. Zhang, and J.A. Renwick, 1995: Dynamic contribution to mean temperature trends. Science, **270**, 780-783.

Wallace, J. M., Y. Zhang, and L. Bajuk, 1996: Interpretation of interdecadal trends in Northern Hemisphere surface air temperature. *J. Climate,* **9**, 249-259.

Wallace, J. M., 1996: Observed Climate Variability: Spatial Structure. In *Decadal Climate Variability: Dynamics and Predictability*, D.L.T. Anderson and J. Willebrand, eds., Springer Verlag. 31-81.

Woodruff, S.D., R.J. Slutz, R.L. Jenne, and P,M, Steurer, 1987: A Comprehensive Ocean-Atmosphere Data Set. *Bull. Amer. Met. Soc.*, **68**, 521-527.

Yamagata, T., and Y. Masumoto, 1992: Interdecadal natural climate variability in the western Pacific and its implication in global warming. *J. Meteor. Soc. Japan,* **70**, 167–175.

Yamagata, T., Y. Shibao, and S.-I. Umatani, 1985: Interannual variability of the Kuroshio Extension and its relation to the Southern Oscillation/El Niño. *J. Oceanogr. Soc. Japan,* **41**, 274–281.

Zhang, Y., J. M. Wallace, and N. Iwasaka, 1996: Is the climate variability over the North Pacific a linear response to ENSO? *J. Climate,* **9**, 1468–1478.

Zhang, Y., J. M. Wallace, and D. S. Battisti, 1997: ENSO-like interdecadal variability: 1900–93: *J. Climate,* **1**0, 1004–1020.

Zhang, Y., J. R. Norris, and J. M. Wallace, 1998: Seasonality of large-scale atmosphere-ocean interaction over the North Pacific. *J. Climate,* **11**, 2473–2481.

3. Pacific Decadal Variability: Modeling

Barnett, T.P., D.W. Pierce, M. Latif, D. Dommenget, and R. Saravanan, 1999a: Interdecadal interactions between the tropics and midlatitudes in the Pacific basin. *Geophys. Res. Lett.,* **26**, 615-618.

Barnett, T.P., D.W. Pierce, R. Saravanan, N. Schneider, D. Dommenget, and M. Latif, 1999b: Origins of the midlatitude Pacific decadal variability. *Geophys. Res. Lett.*, **26**, 1453-1456.

Bladé, I.,1997: The influence of midlatitude ocean–atmosphere coupling on the low-frequency variability of a GCM. Part I: No tropical SST forcing *J. Climate,* **10**, 2087-2106.

Bladé, I.,1999: The Influence of Midlatitude Ocean–Atmosphere Coupling on the Low-Frequency Variability of a GCM. Part II: Interannual Variability Induced by Tropical SST Forcing. *J. Climate,* **12***,* 21-45.

Frankignoul, C., E. Kestenare, N. Sennéchael, G. de Coëtlogon, and F. D'Andrea, 2000: On decadal-scale ocean-atmosphere interactions in the extended ECHAM1/LSG climate simulation. *Clim. Dyn.*, **16**, 333-354.

Giese and Carton, 1999: Interannual and decadal variability in the tropical and midlatitude Pacific ocean. *J. Climate*, **12**, 3402-3418.

Graham, N.E., and T.P. Barnett, 1987: Sea surface temperature, surface wind divergence and convection over tropical oceans. *Science*, **238**, 657-659.

Graham, N. E., 1994: Decadal-scale climate variability in the tropical and North Pacific during the 1970s and 1980s: observations and model results. *Clim. Dyn.*, **10**, 135-162.

Graham, N. E., T. P. Barnett, R. Wilde, M. Ponater, and S. Schubert, 1994: On the roles of tropical and midlatitude SSTs in forcing interannual to interdecadal variability in the winter Northern Hemisphere circulation. *J. Climate*, **7**, 1416-1441.

Hannachi, A., 1997: Low-frequency variability in a GCM: Three-dimensional flow regimes and their dynamics. *J. Climate,* **10**, 1357-1379.

Karspeck, A.R., and M. A. Cane, 2002: Tropical Pacific 1976–77 climate shift in a linear, wind-driven model. *J. Phys. Oceanogr.,* **32**, 2350–2360.

Kawamura, R., M. Sugi, and N. Sato, 1997: Interdecadal and Interannual Variations over the North Pacific simulated by a set of three climate experiments. J. Climate, **10**, 2115-2121.

Kirtman, B. P., 1997: Oceanic Rossby wave dynamics and the ENSO period in a coupled model. *J. Climate*, **10**, 1690-1705.

Kitoh, A., T. Motoi, and H. Koide, 1999: SST variability and its mechanism in a coupled atmosphere–mixed layer ocean model. *J. Climate,* **12**, 1221-1239.

Knutson, T. R., and S. Manabe, 1998: Model assessment of decadal variability and trends in the tropical Pacific Ocean. *J. Climate,* **11**, 2273-2296.

Latif, M., and T. P. Barnett, 1994: Causes of decadal climate variability over the North Pacific and North America. *Science,* **266**, 634–637.

Latif, M., and T. P. Barnett, 1996: Decadal climate variability over the North Pacific and North America: Dynamics and predictability. *J. Climate,* **9**, 2407–2423.

Latif, M., R. Kleeman, and C. Eckart, 1997: Greenhouse warming, decadal variability or El Niño? An attempt to understand the anomalous 1990s. *J. Climate*, **10**, 2221-2239.

Latif, M. and T.P. Barnett, 1994: Causes of decadal climate variability over the North Pacific and North America. *Science*, **266**, 634- 637.

Latif, M. and T.P. Barnett, 1996: Decadal climate variability over the North Pacific and North America: Dynamics and predictability. *J. Climate*, **9**, 2407-2423.

Lau, N.-C., and M. J. Nath, 1994: A modeling study of the relative roles of the tropical and extratropical SST anomalies in the variability of the global atmosphere–ocean system. *J. Climate,* **7**, 1184-1207.

Lau., N. –C., and M. J. Nath, 1996: The role of the "Atmospheric Bridge" in linking Pacific ENSO events to extratropical SST anomalies. *J. Climate*, **9**, 2036-2057.

Lau, N.-C., 1997: Interactions between global SST anomalies and the midlatitude atmospheric circulation. *Bull. Am. Met. Soc.,* **78**, 21-33.

Liu, Z., L. Wu, R. Gallimore, and R. Jacob, 2002: Search for the origins of Pacific decadal climate variability. *Geophys. Res. Lett.*, **29**(10), 10.1029/2001GL013735.

Lysne, J., P. Chang, and B. Giese, 1997: Impact of the extratropical Pacific on equatorial variability. *Geophys. Res. Lett.*, **24**, 2589-2592.

Miller, A. J., D. R. Cayan, T. P. Barnett, N. E. Graham, and J. M. Oberhuber, 1994: Interdecadal variability of the Pacific Ocean: Model response to observed heat flux and wind stress anomalies. *Climate Dyn.,* **9**, 287–302.

Miller, A. J., D. R. Cayan, and W. B. White, 1998: A westward-intensified decadal change in the North Pacific thermocline and gyre-scale circulation. *J. Climate*, **11**, 3112-3127.

Pierce, D. W., T. P. Barnett, and M. Latif, 2000: Connections between the Pacific ocean tropics and midlatitudes on decadal timescales. *J. Climate*, **13**, 1173-1194.

Pierce, D. W., T. P. Barnett, N. Schneider, R. Saravanan, D. Dommenget, and M. Latif, 2001: The role of ocean dynamics in producing decadal climate variability in the North Pacific. *Clim. Dyn.*, **18**, 51-70.

Pierce, D. W., 2002: The role of sea surface temperatures in interactions between ENSO and the North Pacific Oscillation. *J. Climate* , **15**, 1295-1308

Qiu, B., and R. X. Huang, 1995: Ventilation of the North Atlantic and North Pacific: Subduction versus obduction. *J. Phys. Oceanogr.,* **25,** 2374–2390.

Robertson, A. W., 1996: Interdecadal variability over the North Pacific in a multi-century climate simulation. *Climate Dyn.,* **12**, 227–241.

Robinson, W.A., 2000: Review of the Workshop on Extra-Tropical SST anomalies. *Bull. Am. Met. Soc.*, **81**, 567–577.

Saravanan, R., 1998: Atmospheric low-frequency variability and its relationship to mid-latitude SST variability: studies using the NCAR Climate Systems Model. *J. Climate*, **11**, 1386-1404.

Schneider, N., A. J. Miller, and D. W. Pierce, 2002: Anatomy of North Pacific decadal variability. *J. Climate*, **15**, 586—604.

Schneider, N. S., S. Venzke, A. J. Miller, D. W. Pierce, T. P. Barnett, C. Deser, and M. Latif, 1999: Pacific thermocline bridge revisited. *Geophys. Res. Lett.*, **26**, 1329-1332.

Seager, R., Y. Kushnir, N. H. Naik, M. A. Cane, and J. Miller, 2001: Wind-driven shifts in the latitude of the Kuroshio-Oyashio extension and generation of SST anomalies on decadal time scales. *J. Climate*, **14**, 445—466.

Sekine, Y., 1988: Anomalous southward intrusion of the Oyashio east of Japan. I: Influence of the seasonal and interannual variations in the wind stress over the North Pacific. *J. Geophys. Res.,* **93**, 2247–2255.

Vimont, D. J., D. S. Battisti, and A. C. Hirst, 2001: Footprinting: a seasonal link between the mid-latitudes and tropics. *Geophys. Res. Lett.*, **28,** 3923-3926

Vimont, D. J., D. A. Battisti, and A. C. Hirst, 2002a: Pacific interannual and interdecadal equatorial variability in a 1000-yr simulation of the CSIRO coupled general circulation model. *J. Climate*, **15**, 160-178.

Vimont, D. J., D. J. Battisti, and A. C. Hirst, 2002b: The seasonal footprinting mechanism in the CSIRO general circulation models. *J. Climate*, Submitted.

Walland, D. J., S. B. Power, and A. C. Hirst, 2000: .Decadal climate variability simulated in a coupled general circulation model. *Climate Dynamics,* **16**, 201-211

Xie, S.-P., T. Kunitani, A. Kubokawa, M. Nonaka, and S. Hosoda, 2000: Interdecadal thermocline variability in the North Pacific for 1958–97: a GCM simulation**.** *J. Phys. Oceanogr.,* **30,** 2798–2813.

Yukimoto, S., M. Endoh, Y. Kitamura, A. Kitoh, T. Motoi, A. Noda, and T. Tokioka, 1996: Interannual and interdecadal variabilities in the Pacific in an MRI coupled GCM. *Climate Dyn.,* **12**, 667–683.

4. Pacific Decadal Variability: Theory

Alexander, M. A., I. Bladé, M. Newman, J. R. Lanzante, N. –C. Lau, and J. D. Scott, 2002: The atmospheric bridge: the influence of ENSO teleconnections on air-sea interaction over the global oceans. *J. Climate*, **16**, 2205-2231.

Barnett, T. P., D. W. Pierce, M. Latif, D. Dommenget, and R. Saravanan, 1999: Inter-decadal interactions between the tropics and midlatitudes in the Pacific basin. *Geophys. Res. Lett.*, **26**, 615-618.

Barsugli, J.J., and D.S. Battisti, 1998: The basic effects of atmosphere-ocean thermal coupling on midlatitude variability. *J. Atmos. Sci.*, **55**, 477-493.

Bretherton, C. S. and D. S. Battisti, 2000: An interpretation of the results from atmospheric general circulation models forced by the time history of the observed sea surface temperature distribution. *Geophys. Res. Lett.*, **27**, 767-770.

Corti, S., F. Molteni & T.N. Palmer, 1999: Signature of recent climate change in frequencies of natural atmospheric circulation regimes. *Nature*, **398**, 799-802.

Corti, S. & T. N. Palmer, 1997: Sensitivity analysis of atmospheric low-frequency variability. *Q. J. R. Meteorol. Soc.,* **123**, 2425-2447.

Czaja, A. and J. Marshall, 2000: On the interpretation of AGCMs response to prescribed time-varying SST anomalies *Geophys. Res. Lett.* **27***,* 1927-1930.

Deser, C., M. A. Alexander, and M. S. Timlin, 2001: On the persistence of sea surface temperature anomalies in midlatitudes. *J. Climate*, Submitted.

Frankignoul, C., and K. Hasselmann, 1977: Stochastic climate models. Part 2. Application to sea-surface temperature variability and thermocline variability. *Tellus,* **29**, 284-305.

Frankignoul, C., P. Muller, and E. Zorita, 1997: A simple model of the decadal response of the ocean to stochastic wind stress forcing. *J. Phys. Oceanogr*., **27**, 1533-1546.

Goodman, J., and J. Marshall, 1999: A model of decadal middle-latitude atmosphere-ocean coupled modes. *J. Climate*, **12**, 621-641.

Gu, D., and S. G. H. Philander, 1997: Internal climate fluctuations that depend on exchanges between the tropics and extratropics. *Science,* **275**, 805–807.

Hasselmann, K., 1976: Stochastic climate models. I, Theory. *Tellus*, **28**, 473—485.

Kleeman, R. J., J. P. McCreary Jr., and B. A. Klinger, 1999: A mechanism for generating ENSO decadal variability. *Geophys. Res. Lett.*, **26**, 1743-1746.

Kushnir, Y., W. A. Robinson, I. Bladé, N. M. J. Hall, S. Peng, and R. Sutton, 2002: Atmospheric GCM response to extratropical SST anomalies: synthesis and evaluation**.** *J. Climate*, **15**, 2233–2256.

Marshall, J. and F. Molteni, , 1993: Towards a dynamical understanding of planetary-flow regimes. *J. Atmos. Sci.* **50**, 1792-1818.

Miller, AJ., and N. Schneider, 2000: Interdecadal climate regime dynamics in the North Pacific Ocean: theories, observations and ecosystem impacts. *Prog. Oceanogr.*, **47**, 355–379.

Neelin, J. D., and W. Weng, 1999: Analytical Prototypes for Ocean–Atmosphere Interaction at Midlatitudes. Part I: Coupled Feedbacks as a Sea Surface Temperature Dependent Stochastic Process**.** *J. Climate*: **12**, 697–721.

Palmer, T. N. 1993: A nonlinear dynamical perspective on climate change. *Weather,* **48**, 313-348

Palmer, T. N., 1999:A nonlinear dynamical perspective on climate prediction. *J. Climate,* **12**, 575-591.

Palmer, T. N.,1988: Medium and extended range predictability, and stability of the PNA mode. *Q. J. R. Meteorol. Soc.,* **114**, 691-713.

Saravanan, R., and J.C. McWilliams, 1998: Advective ocean--atmosphere interaction: an analytical stochastic model with implications for decadal variability. *J. Climate*, **11**, 165-188.

Saravanan, R., D. J. Vimont, and Z. Wu, 2000: Exotic mechanisms for coupled ocean-atmosphere variability in mid-latitudes. Lecture notes for 2000 NCAR ASP on Decadal and Centennial Climate Variability.

Trenberth, K. E., G. W. Branstator, D. Karoly, A. Kumar, N. -C. Lau, and C. Ropelewski, 1998: Progress during TOGA in understanding and modeling global teleconnections associated with tropical sea surface temperature. *J. Geophys. Res.*, **103**, 14 291-14 324.

Weng, W. and Neelin, D., 1999: Analytical prototypes for ocean-atmosphere interaction at midlatitudes. Part II: Mechanisms for coupled gyre modes. *J. Climate*, **12**, 2757-2774.

Yulaeva, E., N. Schneider, D. W., Pierce, T. P Barnett, 2001: Modeling of North Pacific climate variability forced by oceanic heat flux anomalies. *J. Climate*, **14**, 4027-4046

5. Others

Battisti, D. S., 1998: Dynamics and thermodynamics of a warming event in a coupled tropical atmosphere-ocean model. *J. Atmos. Sci.*, **45**, 2889-2919.

Battisti, D.S. and A.C. Hirst, 1989: Interannual variability in the tropical atmosphere-ocean system: influences of the basic state, ocean geometry and nonlinearity. *J. Atmos. Sci.,* **46**, 1687-1712

Cane, M.A., and E.S. Sarachik, 1981: The periodic response of a linear, baroclinic equatorial ocean, *J. Marine Res.*, **39**, 651-693.

Cane, M.A., and E.S. Sarachik, 1977: Forced baroclinic ocean motions, II: The equatorial bounded case. *J. Marine Res.*, **35**, 395-432.

Chang, P., L. Ji, B. Wang, and T. Li, 1995: Interactions between the seasonal cycle and El Niño-Southern Oscillation in an intermediate coupled ocean-atmosphere model. *J. Atmos. Sci.*, **52**, 2353-2372.

Chang, P., L. Ji, H. Li, and M. Flügel 1996: Chaotic dynamics versus stochastic processes in El Niño-Southern Oscillation in coupled ocean-atmosphere models. *Physica D.*, **98**, 301-320.

Goodman, P. S., 2000: The role of North Atlantic Deep Water formation in the thermohaline circulation. Ph.D. Dissertation, University of Washington, 159 pp.

Neelin, J. D., D. S. Battisti, A. C. Hirst, F. Jin, Y. Wakata, T. Yamagata, and S. E. Zebiak, 1998: ENSO Theory. *J. Geophys. Res.*, **103** , 14 261-14 290.

Schopf, P. S., and M. J. Suarez, 1998: Vacillations in a coupled ocean-atmosphere model. *J. Atmos. Sci.*, **45**, 549-566.

Thompson, C. J., and D. S. Battisti, 2001: A linear stochastic dynamical model of ENSO. Part II: Analysis. *J. Climate*, **14**, 445-466.

Tziperman, E., and M. A. Cane, and S. E. Zebiak, 1995: Irregularity and locking to the seasonal cycle in an ENSO prediction model as explained by the quasi-periodicity route to chaos. *J. Atmos. Sci.*, **52**, 293-306.

Zebiak, S. E., and M. A. Cane, 1987: A model ENSO. *Mon. Wea. Rev.*, **115**, 2262-2278.

WEB SITES:

Climatological Data:

http://ferret.wrc.noaa.gov/las/main.pl (Interactive plotting of data sets)

http://tao.atmos.washington.edu/data_sets/

http://www.coaps.fsu.edu/~grant/reysst/ (movies of Reynolds SST-1981-now).

Patterns:

http://tao.atmos.washington.edu/pdo/

http://horizon.atmos.colostate.edu/ao/

http://www.ldeo.columbia.edu/NAO/

http://www.met.rdg.ac.uk/cag/NAO/index.html